LUDWIG-MAXIMILIANS-UNIVERSITÄT
TECHNISCHE UNIVERSITÄT MÜNCHEN

Institute of Computational Biology
Helmholtz Zentrum Muenchen - German Research Center for Environmental Health

Bachelorarbeit
in Bioinformatik

Quantification of marker expression for endoderm and mesoderm segregation

Sandra Fischer

Aufgabensteller:	Prof. Dr. Fabian Theis
Betreuer:	Dr. Carsten Marr, Michael Schwarzfischer and Dr. Ingo Burtscher
Abgabedatum:	15. September 2013

Ich versichere, dass ich diese Bachelorarbeit selbständig verfasst und nur die angegebenen Quellen und Hilfsmittel verwendet habe.

15. September 2013 _____

Sandra Fischer

Zusammenfassung

Embryonale Stammzellen (ES Zellen) sind der Schlüssel zur Entwicklung des Menschen. Sowohl bei der Bildung innerer Organe als auch bei der Entstehung von Knochen und Blutgefäßen ist alles auf die Differenzierung von Stammzellen zurückzuführen. Für die Entwicklung besonders interessant sind die beiden Keimblätter, Endoderm und Mesoderm, und die damit verbundene Zwischenschicht, das Mesendoderm. Um die Differenzierung von ES Zellen in die jeweiligen Zelltypen, zu untersuchen wurden im Labor von Heiko Lickert die beiden Transkriptionsfaktoren T und Foxa2 mit fluoreszierenden Proteinen fusioniert, und deren Expression während der Differenzierung mit einem konfokalen Mikroskop aufgenommen.

In der vorliegenden Arbeit wurden diese Stammzellen auf Einzelzell-Ebene analysiert und quantifiziert. Zunächst wurden Einzelzellen über bis zu 8 Generationen verfolgt und einen zell-spezifische Stammbäume zu erstellt. Die Einzelzellen wurden dann, basierend auf den Fluoreszenz-Intensitäten, quantifiziert. Um genau festzustellen, wann die Transkriptionsfaktoren signifikant in Zellen expremiert sind, haben wir eine bereits existierende Methode auf einzelne Messzeitpunkte erweitert.

Daraufhin wurden zahlreiche Analysen durchgeführt sowohl bezüglich der Korrelation der Faktoren untereinander, wie auch bezüglich möglicher Korrelationen mit Zellzykluslängen. Dabei konnte keine signifikante Korrelation zwischen den verschiedenen Bäumen gefunden werden, jedoch gab es innerhalb der Generationen einen positiven Effekt. Außerdem wurden verschiedene Ansätze zur Bestimmung positiv expremierter Zellen verglichen und auf Einzelzellen angewendet. Schließlich wurde jede Zelle wurde, nach der jeweiligen positiven Fluoreszenzmarker-Expression klassifiziert, so dass ein spezifisches Muster für jeden Zell Stammbaum erstellt werden konnte.

Abstract

Embryonic stem cells (ES cells) are key to human development. Both in the formation of internal organs as well as in the development of bone and blood vessels, everything can be ascribed to the differentiation of stem cells. Especially interesting for this progress are the two germ layers, Endoderm and Mesoderm, and the associated intermediate layer, the Mesendoderm. To analyze the differentiation of ES cells in the respective cell types, two transcription factors were fused to fluorescent proteins in Heiko Lickert's laboratory, and their expression was recorded over time with a confocal microscope. In the present thesis these stem cells were analyzed and quantified on a single cell level.

First, individual cells were followed for up to 8 generations leading to cell specific genealogies. Also, single cells were quantified, based on their fluorescence intensity. To determine when transcription factors are significant expressed in cells, we adjusted an already existing method to consider single measured time points.

Subsequently analyses were conducted, both for the correlation of the factors among themselves as well as the possible correlation with the cell cycle length. No significant correlation in the various trees could be found, however there was a positive correlation over the generations. Moreover, different approaches to determine whether a cell is positive expressed, were compared and applied correspondingly on single cells. Finally every single cell was classified according their respective positive fluorescence marker expression, so that a specific pattern could be created for every cell family tree.

Contents

1 Introduction

1.1 Motivation

Stem cell research is a controversial field of study. There are many supporters and also a lot of criticism, but one great advantage is obviously: it helps by understanding and healing diseases. In the last year this topic was in media like never before. In 2012, John Gurdon and Shinya Yamanaka successfully discovered a possibility to reprogram induced pluripotent stem cells (iPS-Cell). These cells are having very similar properties like embryonal stem cells (ES cells). Theirs work was distinguished by the Nobel prize.

Then in summer 2013 another important breakthrough has taken place. Scientists from Japan figured out a possibility to create a liver out of stem cells - "To our knowledge, this is the first report demonstrating the generation of a functional human organ from pluripotent stem cells" [21]. Matthew Smalley of Cardiff University's European Cancer Stem Cell Research Institute said: "(This) study holds out real promise for a viable alternative approach to human organ transplants." [21]. One month later scientist from Pittburgh succeeded to establish a heart tissue. As there are not enough organ donors, it is really important to find a way of cultivating organs in vitro.

In May this year a three year old child, from South Korea, got a trachea, created by stem cells. The girl survided only of this transplantation. Paolo Machhiarini inspected a neotrachea seeded with stem cells, he said: "The most amazing thing, which for a little girl is a miracle, is that this transplant has not only saved her life, but it will eventually enable her to eat, drink, and swallow, even talk, just like any other normal child" [43].

The ethical controversy question of stem cell research is smoothed by the new none-ES cell opportunities of iPS cells, based on the two award winners. Does the need of ES-cells is inevitable, Michael Heke, a neurophysiological scientist once said: "The need of embryonal stem cells as model is still required. We need first understand these cells properly to eventually realize the full potential of iPS cells"[39].

1.2 Early embryonic development in the mouse

The primary steps towards the development of the mouse embryo are the formation of the blastocyst, the gastrulation, and lastly the folding.

After fertilization, the single cell embryo is called zygote. During this time the cells of the zygote starts to divide and run through the morula stage (see Fig.1.1). The morula stage consists of a cell cluster, containing between eight and sixteen cells. In this process the volume does not change.

The zygote can be divided into the outer morula and inner morula. The outer morula cells progressively loose their pluripotency and differentiate into trophectoderm (TE), and the inner will form the inner cell mass (ICM). There is though another important part, the primitive endoderm (PE), which creates the border between the ICM (especially the epiblast), and the blastocoel cavity. The blastocoel cavity is formed by the complete formation of the TE. At this time, it is possible to isolate ES cells from the inner cell mass.

The next important part takes place between E 3.5 and E 4.5. First of all, the extra-embryonic (EA) axis is created. There are two hypotheses regarding the EA axis. Firstly, the

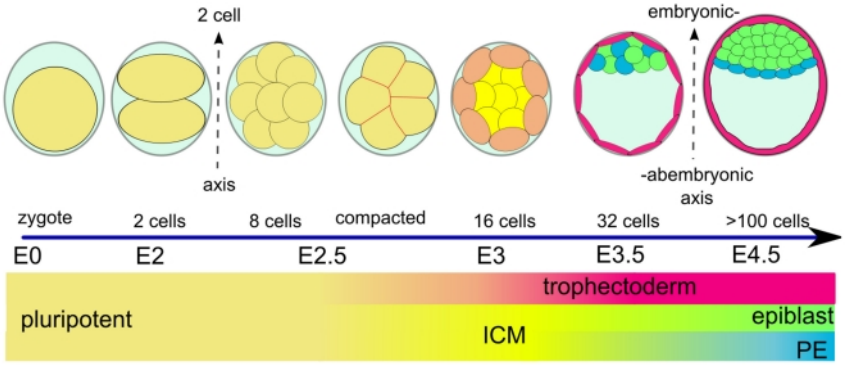

Figure 1.1: The first steps in embryonic development – reaching the blastula stage (image taken from [23]).
After fertilization the zygote starts dividing (E2) and forms the morula (E0-E3) during this stage the cells are pluripotent, that means the cells are now having the potential to differentiate into one of the three germ layers. Cell number is increasing exponential. The outer morula forms the trophectoderm (yellow to pink) and the inner cell mass (yellow) could be distinguished into epiblast (green) and primitive endoderm (blue). Between E3.5 and E4.5 the cells arrange themselves and finally the epilast and the PE are finding there final place.

position of the axis is correlated with the first dividing plan; each of the two daughter cells are able to move to different tissues (TE and epiblast). The second hypothesis is, that the emergence is due to mechanical constraints. Neither is rejected. It is difficult to follow the expansion of cells because of the movement of significant cell and the rotation of the entire cell mass [24]. The other incident during this time of development is the formation of the placenta. Therefore, the blastocyst cells hatch out of the zona pellucida, a protective case around the ovum, and implates into the receptive maternal uterus. Afterwards, trophoblast cells interact with cells from the uterus mucosa and form a tissue which combines maternal and extraembryonic tissues [38]

While the embryo develops, the ICM elongates into the blastocoel cavity, and differentiates into an extra-embryonic and embryonic part (see Fig. 1.2). The embryonic epiblast contains all the progenitor cells, they will contribute to future development. The first morphologic changes can be observed in the extra embryonic portion, while the distal viscerales endoderm (DVE) is formed and moves anteriorly. This leads to a thickening of the VE at the distal tip. The visceral endoderm will be replaced by definitive gut endoderm during gastrulation.

The embryo reaches stage E6.5 and starts with the gastrulation. The gastrulation is the process by which the single layer of the epiblast gives rise to the three germ layers of the ecto-, meso- and endoderm. They are all built from cells of the epiblast [4, 5], by to epithelial-mesenchymal transition on the posteriori side of the embryo. The first step of gastrulation is the formation of the primitive streak on the posterior side of the embryo: Cells from the epiblast undergo epithelial to mesenchymal transition and migate out of the epiblast to form a streak of mesenchymal cells (see Fig. 1.2.) [4, 30]. During gastrulation the Primitive Streak elongates to the distal tip of the embryo. Afterwards the node is formed at the distal end of the primitive streak. The main function of the node is the organizer

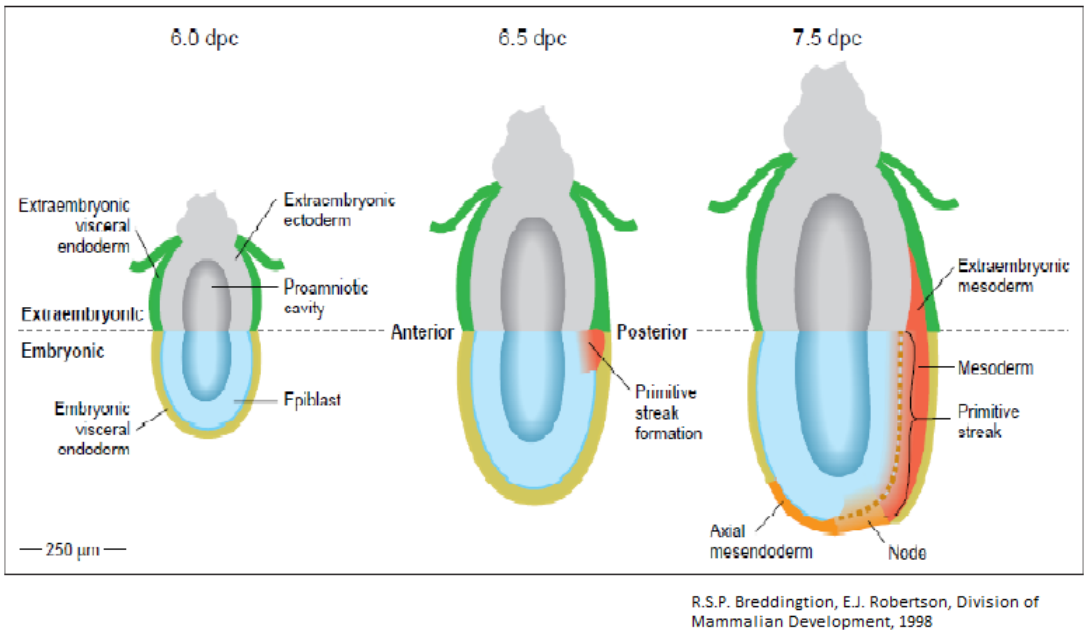

Figure 1.2: Mouse gastrulation (image taken from[4]).
The primitive streak is first evident at 6.5 cpd (days post coitum) which includes the incidence of mesoderm (red). The streak elongates to the tip and the node which gives rise to axial mesendoderm (orange)

function in the late gastrulation stage, providing signaling cues for surrounding tissues [3, 6]. It consists of a dynamic population of cells with different fates. After 7.5 days post coitum, the mesoderm and endoderm surrounding the whole embryo and distal visceral endoderm completely replace the visceral endoderm.

Lastly, there is the final folding of the embryo. After gastrulation, the endoderm is a one cell-layer thick sheet of about 500 cells and represents the outside of the embryo. During the following days, the endoderm is pushed into the inside of the developing mouse and creates a primitive gut tube. This tub will become the gut, and evaginations grows and branches. Passing E9.0, the organogenesis starts [41].

The mesoderm can be divided into four major groups the axial mesoderm, which will give rise to the chorda dorsal, the paraxial mesoderm that segregate into somites. The intermediate mesoderm and the lateral mesoderm. The lateral is subdivided into splanchric and somatic layer. The first one is ventrally and includes the formation of the heart, the main deriviative of mesoderm cells, at that stage. It is associated with the endoderm. The other is the dorsal layer and is associated with the ektoderm. The intermediate forms urgantial apparatus like nephral structures or gonads.

1.3 Endoderm formation

After gastrulation, the endoderm is not determined in regards to its regional fate. The anterior half is already connected to posterior tissues [41]. First, there is the naive endoderm, which is going through many morphological movements until it reaches the formation to the primitive gut tube. The primitive gut tube is surrounded by mesoderm and can be separated into three subgroups: Foregut, Midgut and Hindgut (see Fig. 1.3C). Organs are built by buds growing out of the endoderm epithelium. The result of this proliferation are functional organs [47].

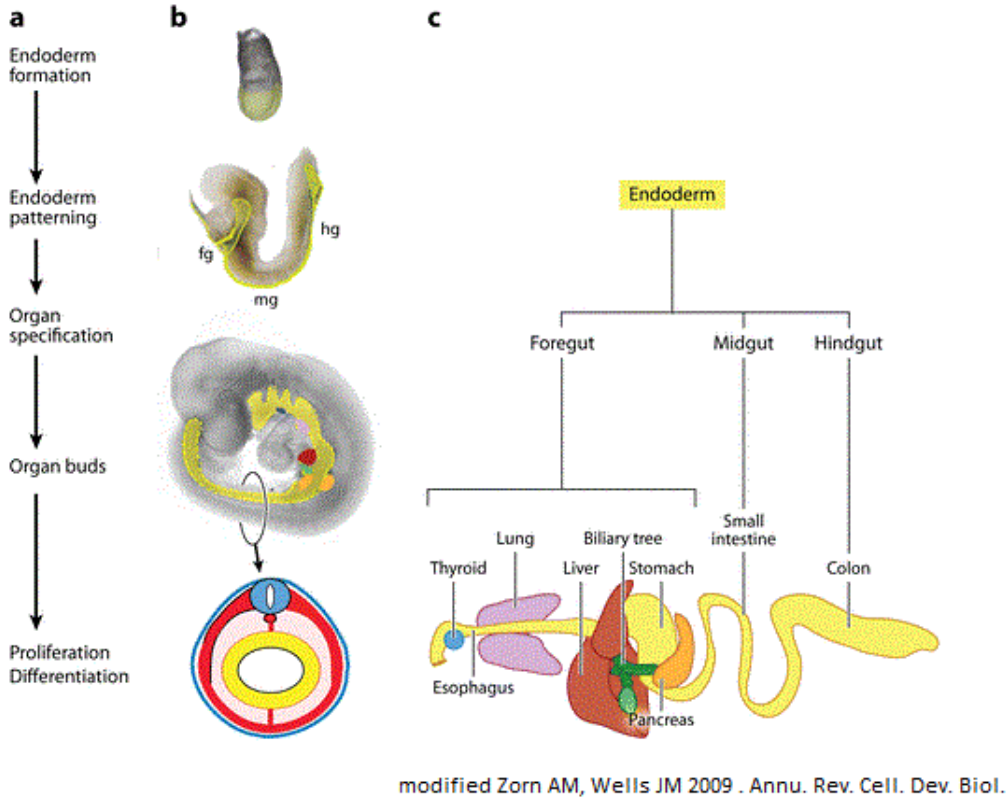

Figure 1.3: Overview and time line of endoderm organ formation (image is taken from [47]). **(a) List of major events in endoderm development including the stages of formation and organ development (b) illustration of time points E7.5 (top), E8.5 and E 9.5 the endoderm is shaded in yellow, surrounding mesoderm is shown (red) and ectoderm (blue). (c) Endoderm cell lineage included the corresponding organs.**

The process of the organogenesis is coordinated by growth factor pathways.

There are two important transcription factors for early and later endoderm development, first the forkhead box transcription factor a2 (Foxa2) and also the SRY-related HMG-box transcription factor 17 (Sox17) .

Foxa2 was first identified in 1991. It turns out that this transcription factor has the ability to bind to regulatory elements of liver specific genes [25]. It is a member of the fox

transcription factor family, which are all having a forkhad box as domain.

Foxa2 is expressed the whole time, from the start of the gastrulation until adult ages [10]. The first expressed factor is Foxa2, later the two very similar subgroup members of the Foxa family are following, starting with Fox1 [2]. Foxa2 is essential for many important genes like, Otx2, which plays a role in the establishment of the anterior-posterior axis and also for the induction of the fore-and mid brain [18, 32]. Another important fact about Foxa2 is its expression during gastrulation. The transcription factor is essential for elongation of the primitive streak and also in the embryonic tissues for the organizer formation. The expression takes part in the epiblast and especially overlaps at the anterior tip of the primitive streak and in the node [20].

Although Foxa2 is compensatory with Foxa1, which is significant for branching morphogenesis of the lung during embryogenesis. These resulted lung cells are type II pneumocytes [37, 28]. Loss of Foxa2 leads to problems with the oxygen supply of the brain during the birth. Transcription factor is indispensable for lung development. Finally Foxa2 is important for organs like lungs, liver and the pancreas. It plays a role in hapatic and pancreatic metabolism and is also essential for generation of dopaminergic neurons in the embryogenesis [46, 26].

1.4 Mesoderm formation

In the early streak stage of the mouse embryo cells ,which are going to build the axial mesoderm, are located in the posterior epiblast. Later they are found at the anterior end of the primitive streak. Cells of the axial mesoderm extend anterior in a tight column along the midline of the embryo, whereas paraxial and lateral cells first migrate laterally out of the primitive streak. Later, they are migrating anterior towards the craniol end of the embryo (see Fig. 1.5.) [31].

Especially, cells from the epiblast move out of the primitive streak and invaginate. Now it is possible, that a few cells transfer to the hypoblast and create the endoderm. The others are between endoderm and epiblast and form the mesoderm. Epiblast and hypoblast are now in contact to the extraembryonic mesoderm until they have overlapped the yolk sac and ammion [14]. Migration of some cells to the midline forms the notochordal plate and especially the trunk forms the notochord, which is important for the formation of the neural tube and establishment of anterior-posterior axis [14].

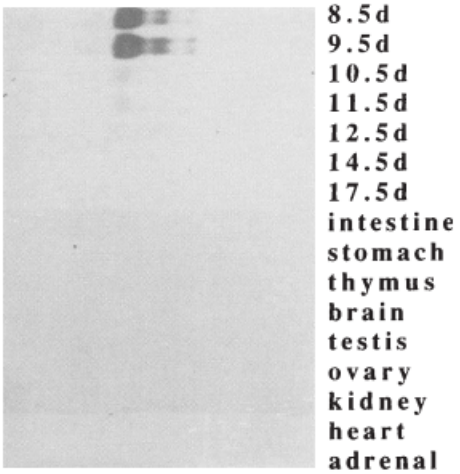

Figure 1.4: Expression of T at different time points and in different tissues (image taken from[42]).
RNA plot analysis from T expression in mouse embryos and adult mouse tissues. Darker gray parts are showing high expression, out of it it can be followed that T is expressed between 8 and 10 days. Later, for 10.5 and 11.5, there is a really weak expression and until day 12 no T is expressed any more.

The last part of the formation of the three
different mesoderm layers is the movement of the mesoderm to the midline, until the whole notochord is sheated. Now, profilerating cells are forming the paraxial mesoderm. The thin layer of every side is the lateral plate and at least the intermediate mesoderm is the middle between paraxial and lateral mesoderm [11].

An important role in the formation and organization of the mesoderm, plays the transcription factor Brachyury (T). It is encoded by the T gene family and was first described in mice [22]. In contrast to Foxa2, which is expressed over the whole time, T is only highly expressed at time points E8.5-E9.5 and looses its intensity by reaching older states and is totally lost in adult tissues. This leads to the assumption that the mesoderm formation happens during this time (see Fig. 1.4.) [42]. Expression is down-regulated to undetectable levels in the paraxial mesoderm and lateral mesoderm. It is expressed in the inner cell mass and the blastocyst followed by the primitive streak and later in the node and notochord. T mutants are not able to provide enough mesoderm, the results are several disruption in morphogenesis from mesoderm derived structures (in particular notochord). It should be mentioned that expression persists in the notochordal plate and definitive notochord, which is the only side of T expression after gastrulation. Mutation leads to notochod malformations and the embryo dies around E9.5. A conceivable explanation is, that the plate is not able to separate from the endoderm [15, 44].

1.5 Embryonal stem cell differentiation

ES cells resemble to inner cell mass from blastula stage. Note, they are still pluripotent, which means they are able to develop into every one of the three germ layers[17]. In 1981, the first murine ES cell line was isolated [27]. In addition to ES cells, there are a couple of other stem cells, like adult stem cells, with restricted differentiation potential, embryonic germ (EG) cells and embryonic carcinoma cells (EC).

To learn more about the development of ES cells, the first step is to observe these cells *in vitro*. Therefore, it is necessary to label the layers of interest, for mesoderm and endoderm. This is possible by using some fluorescence proteins (see section 1.6.). Gain of new *in vitro* knowledge could probably give arise to *in vivo* conditions, and helps to optimize the differentiation of certain lineages *in vitro*. Further observations give rise to some fundamental principles. Under mesoderm conditions, only the transcription factor T (brachyury) is expressed, in contrast to mesoderm, where both T and Foxa2 are expressed [1]. A detailed Q-PCR analysis (see Fig. 1.4.A) shows the expression rate of both genes at different time points, under endoderm conditions. It can be observed, that brachyury reaches its peak during the first time points but increase quickly, and, at the end, the signal is undetectable. Whereas Foxa2 decreases slowly over time and keep the maximum over a longer period. Note the different scales for gene expression, Foxa2 expression reaches a higher value than the other transcription factor. An interesting observation is the comparison of the highest brachyury protein level, after two days of activin A feed (see Fig. 1.6), and the highest expression level one day earlier. Live imaging is a useful method to get a better impression of the interplay of both genes.

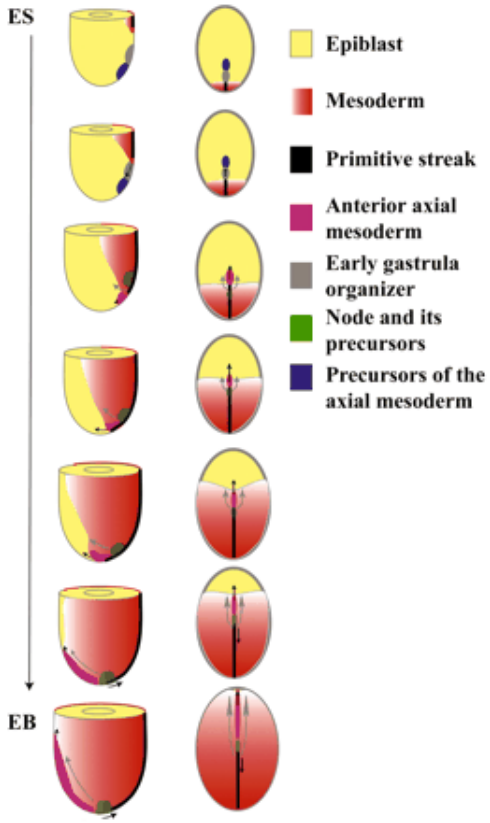

Figure 1.5: Movement of the mesoderm during gastrulation from the early streak to the early bud stage (image taken from [19]).
Left column : lateral view, anterior towards the left; right column: dorsal view, anterior towards the top. EGO (gray) cells move anteriorly with the advancing primitive streak (black) then take a migratory route lateral to the body axis and move with the rest of the cells in the mesoderm to the anterior region of the embryo (pink). Cells leaving the mid-gastrula organizer move tight along the midline of the embryo (black arrow). [19]

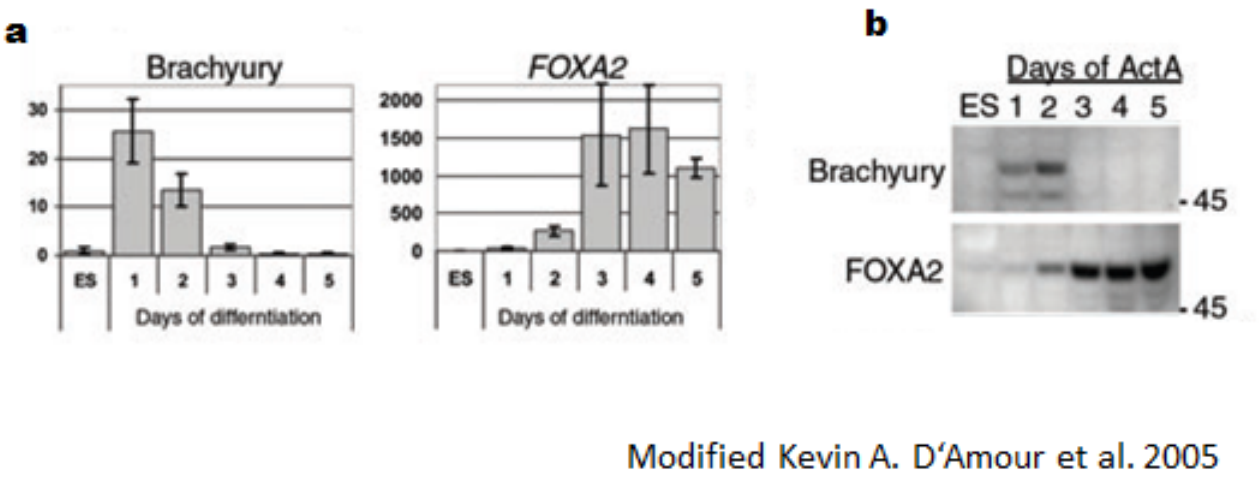

Figure 1.6: Analysis of gene expression under endoderm conditions (image taken from [1]). **a) Q - PCR analysis during 5 day definitive endoderm differentiation for the transcirption factors Brachyury and Foxa2 b) Western Blot : Protein levels for both transcription factors are shown. Darker parts are showing higher expression, therefore Foxa2 is higher expressed during the later days of differentiation whereas Brachyury is more expressed at the beginning. Numbers on the right are position and size (in kDA)**

1.6 Label of endoderm and mesoderm transcription factors

To address the endoderm transcription factor, Foxa2 a reporter gene, Foxa2-TagRFP fusion, was generated [7]. As mice, which are homozygous for the Foxa2 Venus Fusion allele, are viable. Assuming, that the fusion to this fluorescent proteins does not interfere with the Foxa2 function. At closer analysis of every time points of the gastrulation, it was found that the Foxa2 protein and Foxa2-TagRFP reporter are having exactly the same overlapping distribution pattern in nod and endoderm [7].

To incorporate the reporter protein, a targeting construct was created (see Fig. 1.7). The stop codon of the third exon have to be removed, at the same time the open reading is fused to the open reading frame of the fluorescent protein. After this, the actual construct is inserted in ES cells of F1 hybrid mice [16].

To have a marker for the mesodermal population, we used cells with the transcription factor T which are treated with the green fluorescence marker T-GFP. It is targeted to brachyury for detecting the development of the regulated processes for mesoderm. Instead of the fusion strategy for Foxa2, the one for T is a little bit different. Therefore the whole open reading frame of the gene was exchanged with the reading frame of GFP, creating a disruption of the T allele [13]. Now, the allele is disrupted, and the new targeting vector is inserted into mouse stem cells.

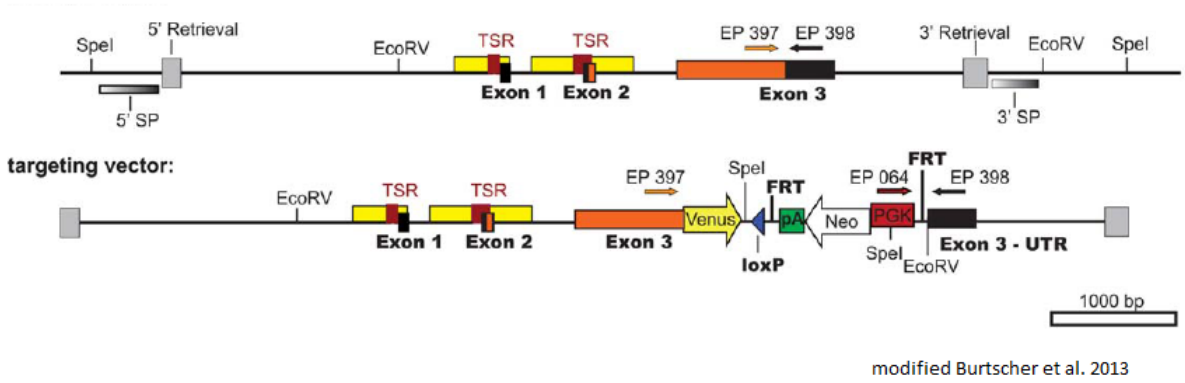

Figure 1.7: Generation of the Foxa2 fusion allele (image taken from [7]).
The wild type allele (top) consists of three exons whereas exon 3 was used to fuse the open reading frame of Foxa2 (orange) to the reporter protein FVF (below vector : yellow)

1.7 The intermediate step - Mesendoderm

The common view, in the field of germ layer formation, is the assumption, that endoderm and mesoderm are sharing a common progenitor state, the Mesendoderm. However, the foundation for this hypothesis is, that both germlayers are emerged at the posterior side of the embryo, at the same time. So far, nobody was able to analyze this differentiation process and follow cells, to generate lineage trees to confirm this hypothesis. It says, that every cell has to go through this stage before reaching its final destination (see Fig. 1.8). Because of this, analysis based on single cell level are necessary to learn more about the process of building the two germ layers.

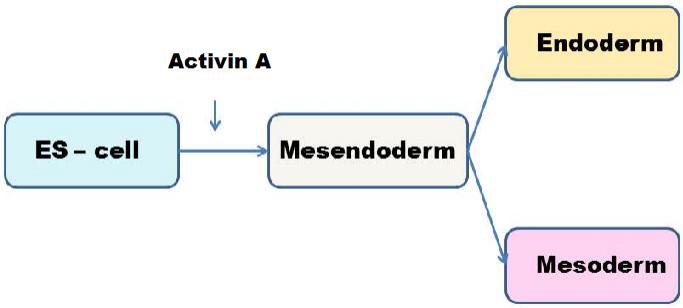

Figure 1.8: Main steps of the ES cell differentiation.
Differentiation of ES cells (blue) are activated by Activin A and is transferred into the intermediate stage the mesendoderm (gray). The mesendoderm can be sepreated into two germ layerns the endoderm (yellow) and mesoderm (pink) [1]

Stem cell research is still a very incomplete research field with many open questions. To characterize the function and meaning of germ layers, it is imperative to look at them in detail. The following chapters, methods and results, describe a comprehensive mesoderm and endoderm study, especially the presence or absence of the indispensable mesendoderm.

1.8 Overview

This work focuses on the behavior of the two transcription factors Foxa2 and Brachyury (T). Nothing is known so far about the correlation between the two factors during lineage specification. The goal os this thesis was to quantify the dynamic of FOxa2 and T during the differentiation of ES cells. We thus tracked and quantified the fluorescence levels of the two colors associated with the two transcripstion factors in movies from the Lickerts lab. In order to make a precise statement about the moment fluorescent marker intensity exceeds a background (and therefore the fused protein is expressed), we extended an existing method to determine a negative gate.

In chapter two, the methods and materials used are described in detail. Both the tools and the data came from the collaboration between the two institutes ISF and ICB, Helmholtz Zentrum München. The analyzed movies were shot in Heiko Lickerts group, while the ES cells and confocal movies were created by Ingo Burtscher [9]. For the cell tracking Timms tracking Tool [12, 33] was used, which was developed at the Stem Cell Dynamic research unit (SCD). A detailed quantification was made possible by the quantification tool QTFy (Schwarzfischer et al. , submitted, Filipczyk et al. s,ubmitted) which was implemented by Michael Schwarzfischer from ICB.

Results from chapter three are based on previously published papers [8, 9, 7]; especially the above described aspects are discussed. Like in previous analyses the differentiation of ES cells was analyzed on a single cell level. The specially developed background correction, which improves the cell specific negative gate, allows a determination of when a cell is expressed a positive signal for one or both transcription factors. Furthermore we observed and analyzed the dynamic relationships of these two important transcription factores."

2 Methods & Materials

In the following sections, the methods for getting the best impression of embryonal stem cell behaviors under in vitro conditions, are explained. Starting with taking live imaging movies and continuing with cell tracking and further quantifications. A few positions, which in this case mean the recorded field of view, are selected to create a family cell tree, so every single cell can be validate with tools written particularly for this purpose. For a better validation we introduced a method, to correct the background noises and determine whether a cell induces a real signal. Further results are showing, that the background noise is regularly above zero and so there are some noises in the background, which have to be regulated. As opposed to earlier developed background correction tools, there is no longer a position specific background noise. Furthmore the difference to previous published methods, is the distribution of background pixel in the images. Resulted from different microscopy techniques, there is no distinction between intensity values in the middle of one image to values at the edge of an image. Therefore a new algorithm for these kind for interferences is needed.

2.1 Live imaging via confocal microscopy

We employed live imaging to visualize the germ layer formation. One opportunity is to make a movie by using a confocal microscopy, a special kind of light microscopy. The difference to conventional light microscopes is the way the pictures are taken. A laser illuminates a single dot at a time point, and the reflected light only detects a single focal plane and converte them to a gray scale value. For a picture of 1000 x 1000 pixel, this happens 1000000 times, this means there is not one picture of the whole sample at any time. The laser light is emitted and fluorescence proteins will be able to absorb the energy of that light and reach an excited state. Then the light is emitted again, but now with a higher wavelength (fluorescence), which will be detected by the microscope.

One important fact of confocal microscopy is the recording of stacks. Stacks are visual sections of the sample. It is caused by a small pinhole where only light of the sharply imaged part of the sample is transmitted. Light of other surrounding planes is blocked and will not be detected. So, the user is able to map many different planes of the sample and so reconstruct the three dimensional structure. For the quantified movies, which are described in the subsequent text, we used just one stack with a high volume, so that the laser detected mostly the whole cell. Furthermore, this technique of microscopy providing an high resolution.

For sure, a lot of preparation is necessary to start a movie, an establishment of static embryo culture system and also a fluorescence marker proteins in transgenic animals. First of all, cells were seeded on a specific layer, including a colloagen-coated surface. The growth medium is supplemented with several chemicals including activin, which is important for proliferation [36]. A lot of experiments are showing cell apoptosis during activin absence. But there is a difference of cell death, in high culture density (10^5ml) a few cells survive and possibly proliferate [45].

After six days the cell cultrure is labeled with BrdU, a chemical bond which will label proliferated cells, and then stored on ice. The minus degrees will keep off the progression of

the cell cycle. To collect mesoderm and endoderm cells a sorting method (FACS-Fluorescence activated cell sorting) is used and later the chosen cells are fixed in 75% ethanol. After washing and incubating, the culture is placed under the microscopy lens.

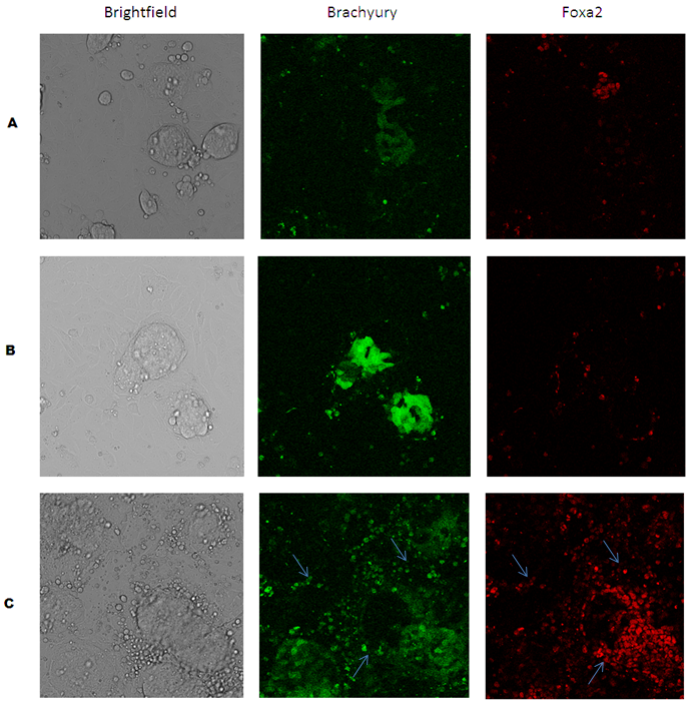

Figure 2.1: Confocal microscopy images

Images from live confocal microscopy with three channels: brightfield, T with fluorescent marker T - GFP, Foxa2 with fluorescent marker Foxa2-TagRFP. All images are from one movie. A) position 19 time point 122 (20,3 h) some overlap in T (green) and Foxa2 (red) B) position 8 time point 216 (36h) green fluorescence is dominating C) position 35 time point 196 (32.6 h) a lot of dead cells can be observed - see blue arrows in C.

After a few main settings, the interesting positions, meaning the field of view, are analysed. These are mostly 30-40 positions, which are all containing a cell colony. It is important to locate the field of view in the middle, otherwise it is possible that some cells are out of focus, which is a result of cell movement and growth. Then the different markers get a specific wavelength (see Fig 2.1.) and the recording is started. The time span may be selected, here the movie runs for 48 hours (two-day-movies).

Once the time is over, the single pictures are available for analyzing. Movies made under mesoderm conditions (see Fig. 2.1.B) are only expressing T, the Foxa2 signals are coming from dead cells. It is important to compare both fluorescence channels with the brightfield channel. Dead cells sometimes lead to wrong assumptions (see Fig 2.1.C) and perhaps cells are classified as double positive cells. Dead cells can be identified by looking at the brightfield channel, they are round cells with distinct boundaries. In the different wavelength channels cells with high auto fluorescence are also corresponding to dead cells, therefore the intensity value of both channels is nearby the same. The possibilities for two different types

of differentiation can be observed under endoderm conditions (see Fig. 2.1. A). On one hand, there are double positive cells, which means they are although T and Fox and, on the other hand, there are single positive cells, expressing only T or only Fox.

By comparison both channels, the different types of used markers can be be recognized. The green fluorescent marker T-GFP is a cytoplasmic marker by contrast to the other marker, which is expressed in the nucleus. The boundaries of a cell are better to distinguish by the nuclear marker, whereas the cytoplasmic boundaries are blurred. For a better and more accurate cell analysis, a third marker, a cyan fluorescence protein fused to the histone subunit 2B (H2B-CFP), is introduced (see Fig. 2.2).

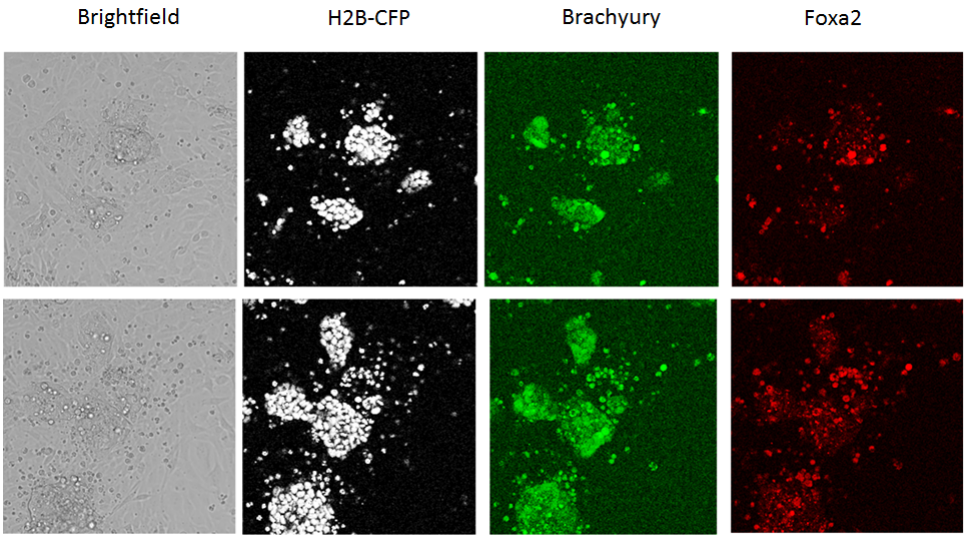

Figure 2.2: Confocal microscopy images with deliberately marker.
Images of confocal microscopy with four channels: brightfield, nuclear marker for better analysis, T with fluorescent marker T-GFP, Foxa2 with fluorescent marker Foxa2-TagRFP. Two different positions both at time point 87 (14,5 h).

The recently introduced marker facilitates the cell tracking. Now it is possible to observe one cell from the beginning of the movie, and not only when a light signal is clearly enough to recognize it by eye.

In the next section, all analysis and quantification are based on these two movies (see Fig. 2.1. , Fig. 2.2. and Table 1). These movies are made by Ingo Burtscher, a movie made by myself is inoperable because of too much cell death, which is probably caused by issues with the cell medium.

2.2 Cell tracking - Timms Tracking Tool

Timm Schroeder (Stem Cell Dynamic research unit (SCD)) developed a tool which enables to follow cells over a long period of time [12, 33]. With the aid of this tool, called Timms Tracking Tool (TTT), cells are analyzed at the single cell level. TTT provides a intuitive and intelligible layout with two various graphic windows. By selecting a position, a movie window will open, where the whole movie, individually for each channels, is shown. There is also the possibility to choose one overlay sub-window where all different channels are shown together. The second window displayes the tree from each tracked cell.

Before starting the tracking, all recorded positions have to be split into single images and renamed, so that the program is able to get the right information for channel identification and time point classification. I manually tracked several positions to generate a representative data set (see Table 1), TTT's automated tracking approaches will fail for this kind of movies. While circling the cells, just by holding the cursor over the required place, the tree in the other window will grow (see Fig. 2.3.). The program also offers the possibility to choose out of many different cell specific properties. The most important are the possibilites to highlight cell division and cell loss.

As discussed previously, it is not easy to identify the boundaries using T-signal cells, and the brightfield is also not helpful (see Fig. 2.1.A and Fig. 2.3), which is a result of the recording of three dimensional colonies (see section 2.1.). While tracking each single cell, a tree growths and represents all divisions by individual branches (see Fig. 2.3B,C). The user has also the possibility to annotate the lines with specific colors to identify single and double positive cells in a qualitative way, question marks at the end of one branch simulate cell loss. For the other movie, the one with the additional nuclear marker, another more channel window is depicted.

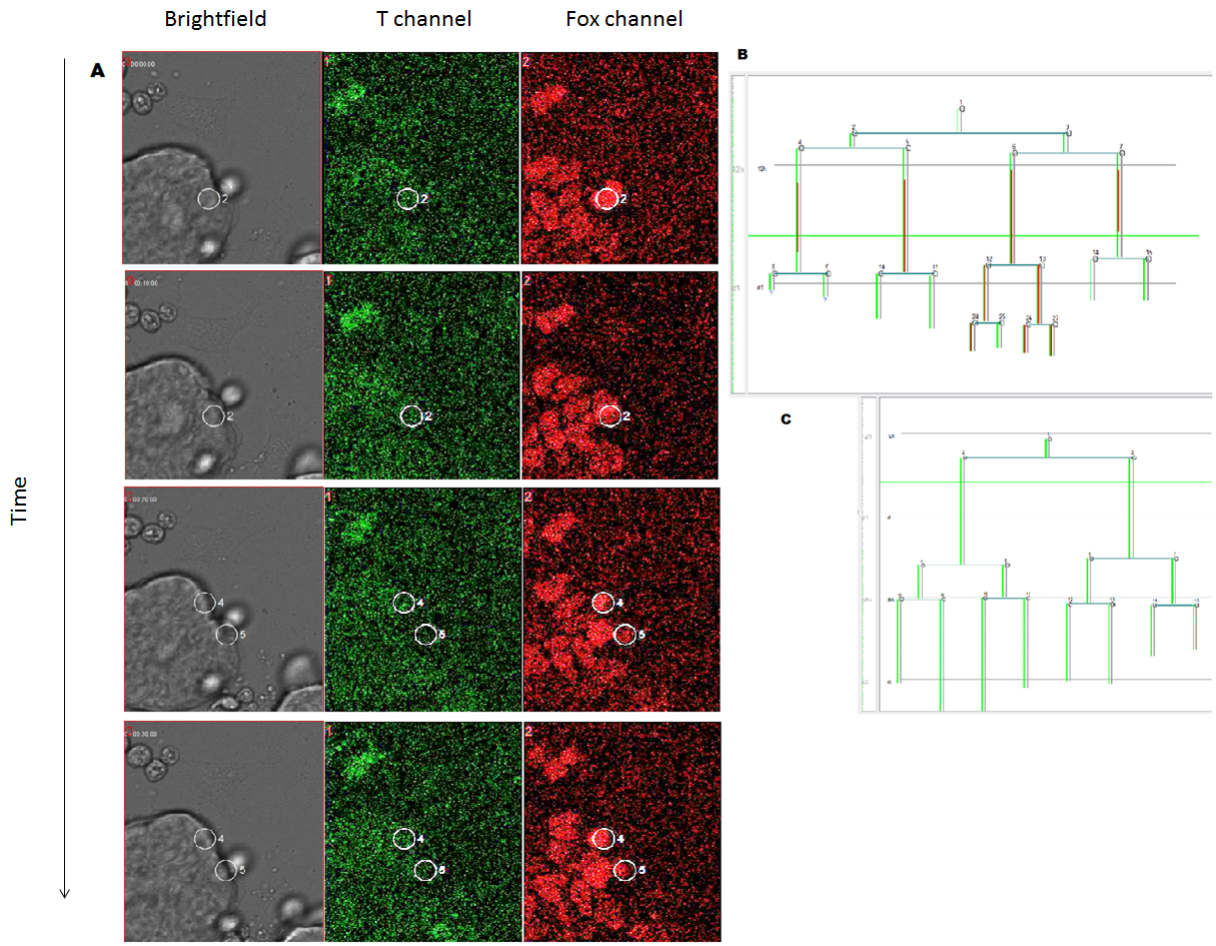

Figure 2.3: TTT illustration of the graphical interface.
A) The way to illustrate a cell division with Timms Tracking Tool, the three channels (bright-field, T and Fox) are separated into three different sub windows. The tracked cell is the second, which is illustrated by number two next to the circle, and cell two will divide into cell three and four.
B) One complete tree the two colored lines demonstrate the double positivity of T and Fox (green and red line) in a quanlitative way .
C) One complete tree which is only positive for T (green line).

Tracking all positions and cells of interesent, a lot of time has to spend but it is the only way to get a detailed overview of the behavior of cells during differentiation. Doing it manually is more exact, but there are probably many other mistakes. Manually tracking is a biased tracking because of the individual influence, like the conception of a real signal. The results are probably overlooked signals and perhaps another observer will track different cells. Also the possibilities for adjusting the wavelengths signals, will probably lead to wrong interpretations.

2.3 Quantification of trees - Quantify tracked fluorescence tool

After tracking all positions it is necessary to analyze and quantifiy the cells. To get a better overview of the cell properties, a quantification tool, called QTFy, was developed by Michael Schwarzfischer from the institute of Computational Biology (ICB). The program works with the TTT-trees and also the microscopy images are needed, to detect every single cell. This quantification is based on the earlier tracked results, and generate automatically the fluorescent intensity of every cell over all time points (see Fig. 2.4).

Figure 2.4: Time courses of calculated marker expression by QTFy.
QTFy time courses: first row belongs to the T marker expression and the second row to the Foxa2 marker expression, the figure belongs to the first movies without extra nuclear marker. Different colored lines simulate different cells resulting from divisions. The y-axis shows intensity value and the x - axis each time point. Last row came from TTT tracking and just reproduce the tracked tree, colors are choose randomly and does not give advise to which kind of marker is expressed.

Because of the better cell distinction of a nuclear marker, both channels were detected on the Foxa2 images. Normally, the program was written for quantification of blood cells, which are small round cells mostly without any cell overlap and also for ES-cells, but therefore the cells were flat and broad. For that kind of cells, the tool works very well (Hoppe et al. submitted), but for detecting these ES cell movies, it was not easy to figure out single cells (Filipczyk et al. submitted). The automatic detection does not work very well and we had to use the two alternative ways. First the program offers the possibility to segment cells by using an ellipse, the other way is to segment cells by drawing freehand circles. Even the freehand option does not provide a perfect quantification. During the absence of Foxa2

signals, it is only possible to segement cells based on the cytoplasmatic T marker. This is difficult and sometimes impossible to segment one cell.

After quantifying every cell manually, the tool provides not only the visualization of time courses but also a detailed output file. This file includs informations like: cell area, exact time point, intensity and cell number; which appropriate all relevant information's for further analysis.

Note that the intensity level of various rows might be different and an equal comparison is sometimes not possible.

	Set 1	**Set 2**	**Set 3**
Tracked positions	9	2	1
Total number of trees	10	15	47
Total number of cells	379	59	103
Movie length [h]	24	16	16
Total measurements (one channel)	6152	2880	6300
Unbiased set	x	x	✓
Used marker	T – GFP, FRF	T-GFP,FRF, H2B-CFP	T-GFP,FRF, H2B-CFP

Table 1: Summary table of three data sets.
Set 1 corresponds to a two-day movie with two fluorescence markers; Set 2 and Set 3 correspond to a shorter movie including three fluorescence markers. Tracked positions are only those positions that contain differentiation. In both movies always more than one position is recorded and furthermore in one position multiple trees can be traced. The total number of tracked cells include cells that died and are lost.

To analysis the data, three different data sets were constructed and all methods from chapter two were applied on them (for a detailed overview see Table 1).

- First data set contains ten trees from nine different positions. One advantage of this set is a long movie length with many cell divisions. In this case only two fluorescence markers are used, the green marker T-GFP and the one which marks the Foxa2 differentiation. Disadvantages of this set are, that the data is possibly inaccurate because of the cytoplasmic marker and so it is not definite that all cells and divisions are true.

- Second data set is only based on two positions and is shorter than the first one. Because of the short movie lengths only a few cell divisions were recorded, in most cases just one division per cell. The advantages are the additional nuclear marker, which provides a more accurate and also faster way to track cells. The quantification tool segments only this marker and the results are more representative. The disadvantages are a high number of cell deaths during the movie and only a few cells differentiate. Just two of all recorded positions are containing cell colonies, including a positive marker expression.

- At least a big set of every cell from one position was tracked, this unbiased tracked set corresponds to the short movie with the additional nuclear marker. Cells with neither T or Fox differentiation are also tracked, and some cells are not going to divide during the movie. This set is a good way to study the behavior of stem cells, it is possible to figure out at which time points one marker passes the stage of beeing positive. Also the question of marker correlations could be answered. Another point is the possibility of making a statement about how many cells are positive during the whole time. Like before the problem is cell death, because of this the tracking is interrupted and a lot of unfinished trees are the result.

2.4 Background correction and negative gate

As already seen in the figures above (such as Fig.2.2.), there is not only a fluorescence for positive cells but also a background signal. This background noise probably lead to a wrong result of cell intensities, and it is inevitable to find a solution to solve this problem.

2.4.1 Global negative gate

One first idea was to implement a function, which calculates one position specific gate. All values above the gate are real signals and these under the line represent a wrong signal which is lower than the background. The aim is to determine something like an simulated cell distribution, only built by background pixel. The difference to earlier developed methods, (Hoppe et al. submitted) is the incidence of background noise in the middle and at the edge of the images. Because of the use of a confocal microscopy (see section 2.1.), there is no curvy lens and the background pixels are the same, independent of the position of the background sliding window. The following enumeration explains the main steps of finding such a cell.

1. First, we determine a set of cell sizes. By selecting, all cell sizes from one position (see Fig. 2.5.A). It is not the aim to calculate the gate by a specific selected cell size, so one random area is chosen.

2. Then a 100 x 100 pixel window of the image, containing only background signals, must be defined. Based on this small window, a collection of intensity values for further use is generated (see Fig. 2.5B). The gaps between the bars are a result of the recorded movies with an eight-pixel depth.

3. The next step is one of the main parts. If n is the randomly chosen cell size, and p is one randomly chosen intensity value from the background collection, then the algorithm picks n times p random values and sum them up (see Fig. 2.5.C). The result is then one specific value (D) which represents the intensity of one simulated background cell with size n.

4. Step 1-3 is repeated a 1000 times (see Fig.2.5.E), so a big set of position specific background cells is simulated..

5. At least a 99%-quantil is calculated and delivers a value which will be the negative gate for this position. Every cell intensity above this gate is positive with 1% false positive rate.

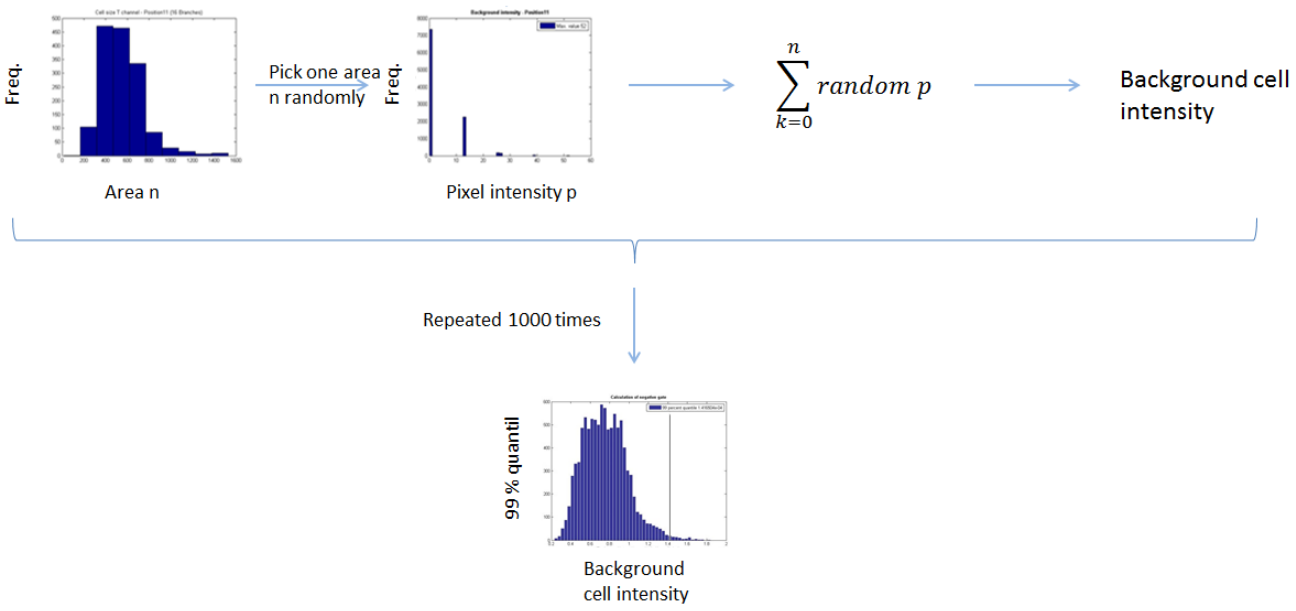

Figure 2.5: Workflow of global gate calculation.
Stepwise deceleration of creating a global gate. A) histogram of area for tracked cells B) intensity value from background C)D) creating a cell for an randomly chosen area E) to get a collection of imaginary cells the steps A-D are repeated several times.

To extend the described method, background correction can be implemented additionally. Like before, one 100x100 pixel window is selected and the mean of these pixels is computed. This mean value gives information about the average background noise and should be a value slightly above zero. Afterwards the mean value is subtracted from every single intensity value of the whole movie, including those with no signal. It is possible to get some negative intensities. Steps 1-5 are applied on the new calculated intensity values, at least the expected gate should be much smaller than the one without background correction, due to somenegative values. This more sophisticated method is a much more accurate possibility to determine wheather a cell is positive or not.

2.4.2 Specific negative gate

In the previous section, one negative gate with a global value for all cells was explained, now an advaned method is introduced: the specific negative gate. The main difference to the global gate is the use of a cell specific gate, in contrast to a position specific gate. Individually the following work steps are an improvement of the global gate.

1. The first difference to the other gate is the stimulation of the cell size. For each cell at every time point, one individual cell size is appropriated for further computations (see Fig. 2.6.A,B).

2. The next steps are similar to the steps above (steps 2-3) random intensities are summed up to built a simulated cell.

3. At this time, there is one value for one background cell with a specific cell size. But the aim is to calculate a cell which represents a background cell as accurately as possible, so the process is repeated a thousand times until a set of fictive cells exists. Notice, the repetition is only performed with the specific cell size n (see Fig. 2.6..D)

4. Getting one cell specific negative gate, again a 99% quantil is applied to the simulated background cells.

5. The aim is to calculate the negative gate of every cell, so the whole process is repeated with the next cell of time point $j+1$. Notice, there is no need to compute already calculated cell areas again.

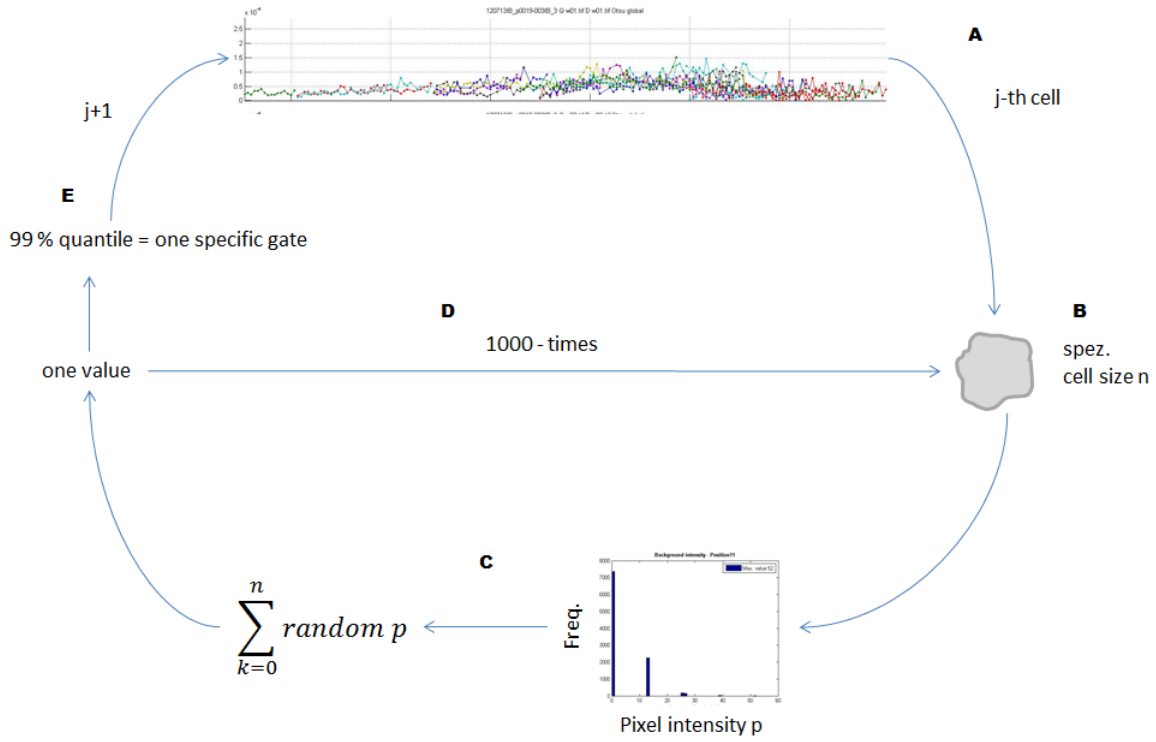

Figure 2.6: Workflow of specific negative gate algorithm.
Stepwise illustration of the computation of a specific negative gate. A) whole collection of every single cell, where one by one a size is selected (B). Based on selected size a background cell is calculated by randomly chosen background intensity values (C) and delivers one value. The cell generation steps are repeated (D) several times and led to a set of imaginary cells for size n. A 99 percent quartile (E) is applied and the gate for cell j is computed. Steps are repeated for each j cell.

The advantages of a specific negative gate are obvious, many different cell specific factors are included. Also for this method there is the opportunity to add a background correction. The process is the same like that of the global gate by subtracting a mean background value.

Another advantage of a specific gate is the ability to give an exact statement about a positive or negative cell signal. By visualizing these results, someone is able to read the gate out of the illustration.

3 Results

With the help of the specific negative gate, further analysis can be applied on the movies from the ISF, to get a better impression behavior of Foxa2 and braychury. Therefore, especially the correlation between the two transcription factors is analyzed. Particular attention is paid to the time points when one of a fluorescent marker is showing a positive signal. Further analyses are made to figure out if there is a correlation between the two markers or between marker expression and cell cycle lengths. The following statistical tests are all performed on background corrected cells including the knowledge of the specific negative gate. The analyses focus especially on the length of the cell cycle and its interaction with a respective expressed marker. Also we found patterns of marker expressions for each tree, and therefore for each branch, and are going to describe them in detail.

3.1 Background correction and negative gate

For a better result, the background correction from chapter 2 is applied to all sets (see described sets in 2.3.). To get an expression which of the three different negative gate approaches is the most effective, they were all applied on the data sets. In the following results, corrections and negatives gates are shown on one tree, this tree corresponds to set 1. The tree is showing some cell divisions and a high increase of maker intensity for one cell. Every method is applied to this tree and we are going to didcuss the results in detail.

The first and simplest way is a global negative gate without background correction. A in silico background-cell distribution is calculated and the 99% quantil represents the negative gate (see Fig. 3.1). The corresponding value of the 95% quantile was too low and with the chosen, quantil 99% quantil, only a 1% false positives have to be accepted. Resulting differences of the distribution including background corrected cells are showing a shift of the curve towards the negative intensity values (see Fig. 3.1.B) Also a more smoothed normal distribution occured, which is caused by more similar intensity values.

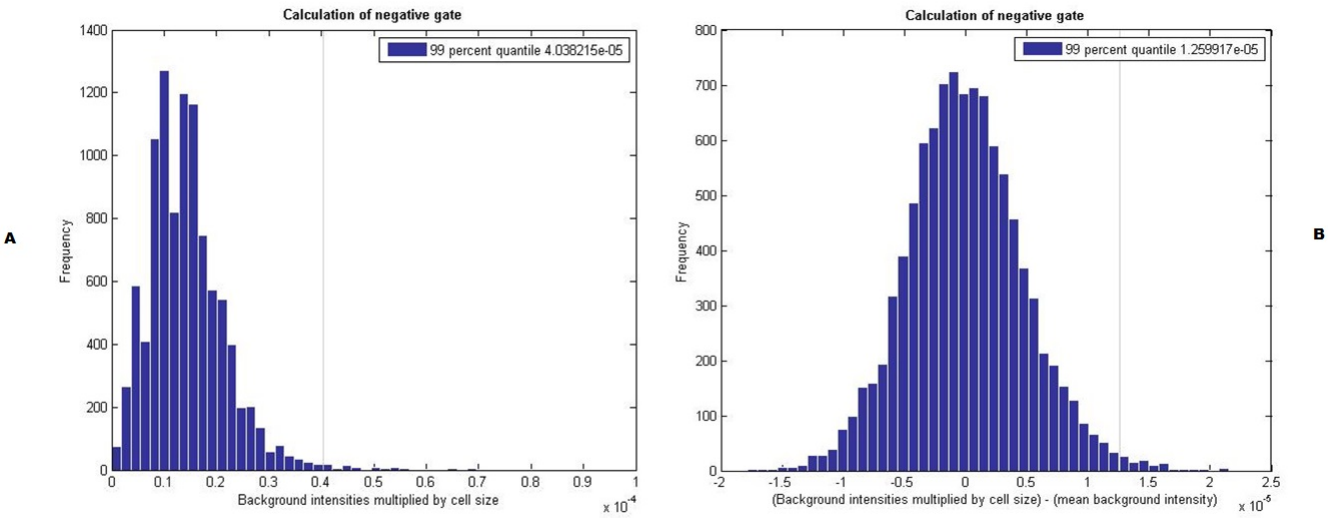

Figure 3.1: Distribution of background cells - without and with background correction.
A) Histogram of 1000 simulated cells computed with random cell size and background intensities (for Fox). Grey line shows the 99%-quantil which is $4.03 * 10^{-5}$**.**
B) Histogramm belongs to the same position but every cell intensity value is substrated by the mean background intensity value, from this it follows that, they most values should be saround zero and it is also possible that some are negative. The 99% - quantil is lower than before $1.25 * 10^{-5}$**.**

In the next step, this quantile is drawn in the QTFy time course to get a threshold for negative or positive cell signals. Such a gate is computed for every channel individually (see Fig. 3.2).

The T channel is mostly positive, but some cells fluctuate between the two states and it is unclear to determine which cells are negative and which are not. At first glance, the second row seems to be wrong. One expects that cell 13 (black line) is positive because of the high increase. Note that the different signals are very weak, compared to the others, and, therefore, it is possible that a apparently bigger differences in the cell lines is still only background noise. To get a better impression of this tree, some microscopy images for several time points are shown (see Fig. 3.2.A). Now it is not easy to give a statement about the quality of the global gate, the comparison to the other computed negative gate is needed.

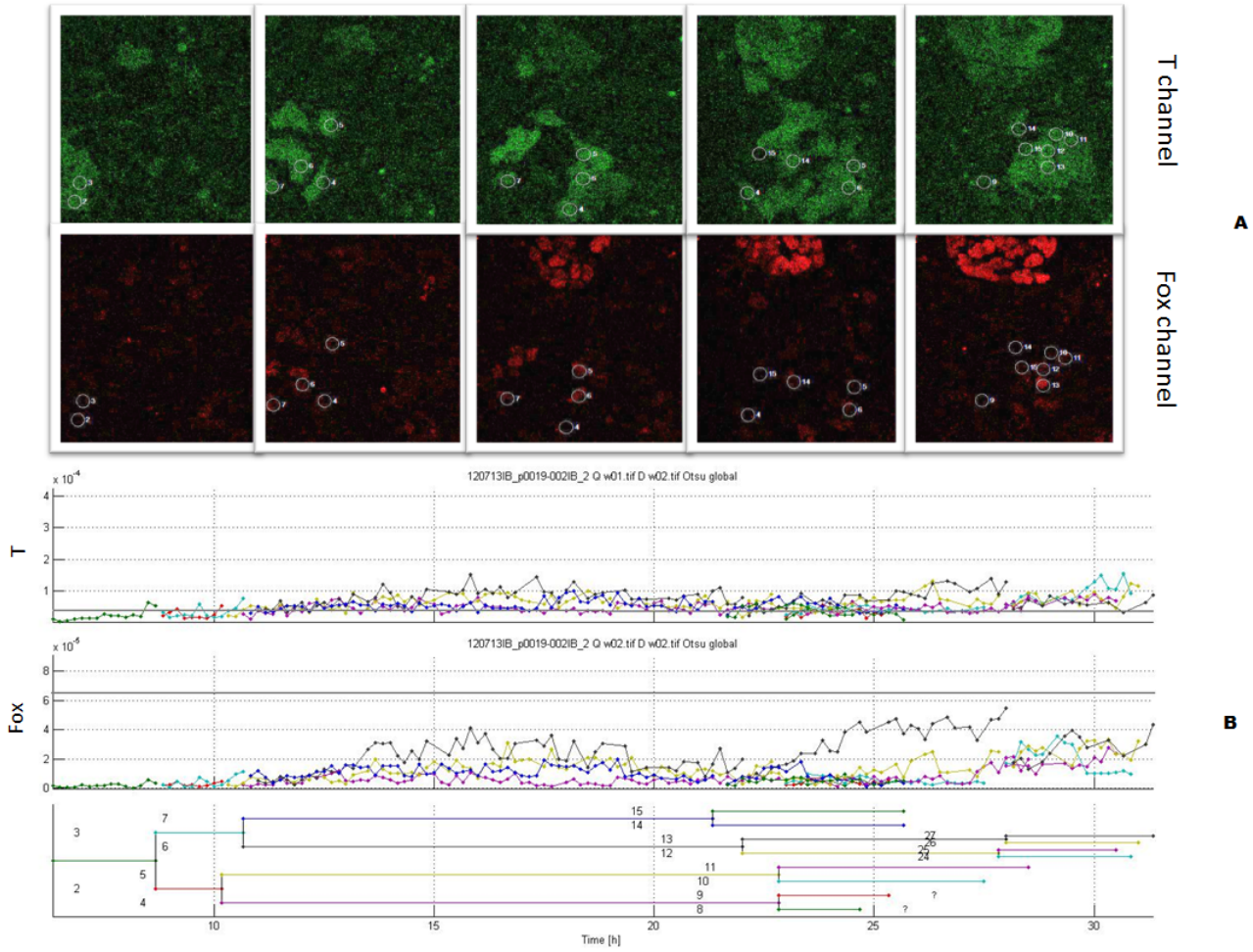

Figure 3.2: QTFy time courses with a global negative gate.
A) Images of both channels at several time points.
B) QTFy time courses : first row represent T intensities and second row Fox intensities. The vertical gray line is the calculated global negative gate - all cells above are a real signal, here for Fox there is no positive signal and T is most of the time positive.
Global negative gate: T $= 0.41 * 10^{-4}$ **Fox** $= 6.48 * 10^{-5}$

Because of that reason, the global gate with background correction is generated for the same tree (see Fig. 3.3). Immediately, a few differences can be observed, especially for Fox. Note, the different intensity distribution for both fluorescence channels, the values are much lower then before, which is a result of correcting every single cell by subtracting the mean background noise.

The true positive cells, which are showing an expression in T, are related to the result from the method above. Over all there are more positive cells and the marker turns on at the same time (time point seven), but the two daughter cells are positive, from the beginning. By contrast the two daughter cells from above are showing no signal after dividing and slowly the intensity value increase. The rest looks very similar in both methods. The gate for Fox looks more different, in contraste to the other Fox-gate, few some cells are positive and a lot

of cells are very close to the gate line. One cell (cell number thirteen) is obviously positive and by comparison with the movie (see Fig. 3.2.A) this cell seems to have a real signal, showing a viewable higher expression. This method seems to be better than the one without background correction, but this begs the question, if this gate is critical enough or if too many cells are incorrectly labeled as positive ones. Remember, the shown pictures are all adjusted 80% brighter and they are all having a higher contrast. Without adjusting, the signals are too weak to be visible to the eye. Not only the tracked colony is shown in the images, but also one colony with a really high Fox signal. This signal indicates a real positive expression, and the tracked colony, for the greatest parts, probably not.

The global gate brings the conclusion of a moderate method. The quality is not satisfying and another more accurate method is needed, but it also gives first exposures of advantages and disadvantages. A gate is needed, which is more critical than the global gate with background correction. This leads to the first conclusion that a background correction is necessary but in a more specific way.

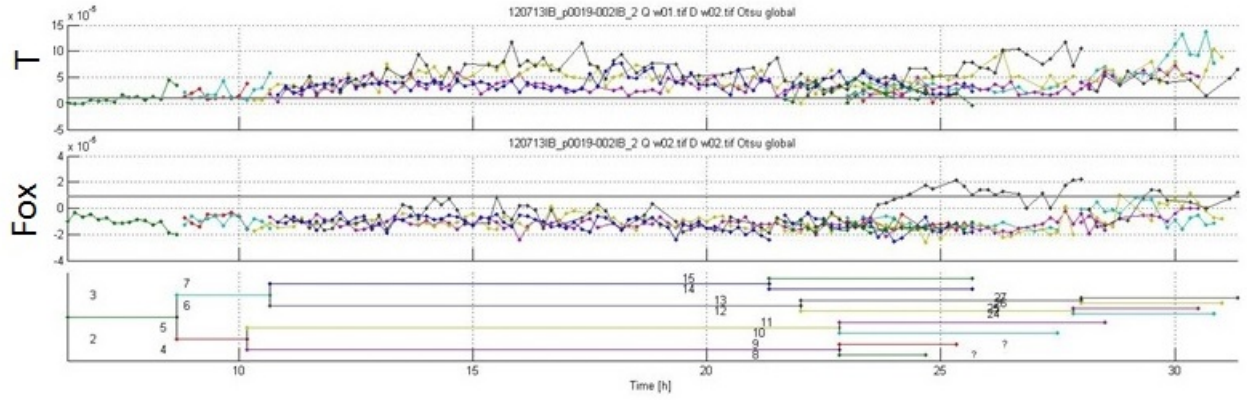

Figure 3.3: QTFy time courses with global negative gate including background correction.
QTFy time courses: first row represent T intensities and second row Fox intensities. The vertical gray line is the calculated global negative gate with background correction - all cells above are a real signal. All T signals and a few Fox signals are positive. The intensity distribution is adjusted and corrected, by substrating the mean background noise for every single cell (so the intensity values are probably negative).
Global negative gate: T $= 1.1 * 10^{-5}$ **Fox** $= 1.23 * 10^{-5}$**.**

Next the third method, the specific negative gate (see section 2.4.), is applied. Because of the previously described advantages of a background correction, the specific negative gate is now always computed after background correction. Now the gate is calculated individually for every single cell, but one has to pay attention by comparing these cells. Maybe there a great differences in cell size, probably resulting from biological issues or because of inaccurate segmentation. Thus greater or smaller background cells are computed. It is possible, that a big cell is positive, just because of its enormous size. To get a better overview about the gate and the corresponding cell areas, an area-time-course is plotted, too (see Fig. 3.4.C).

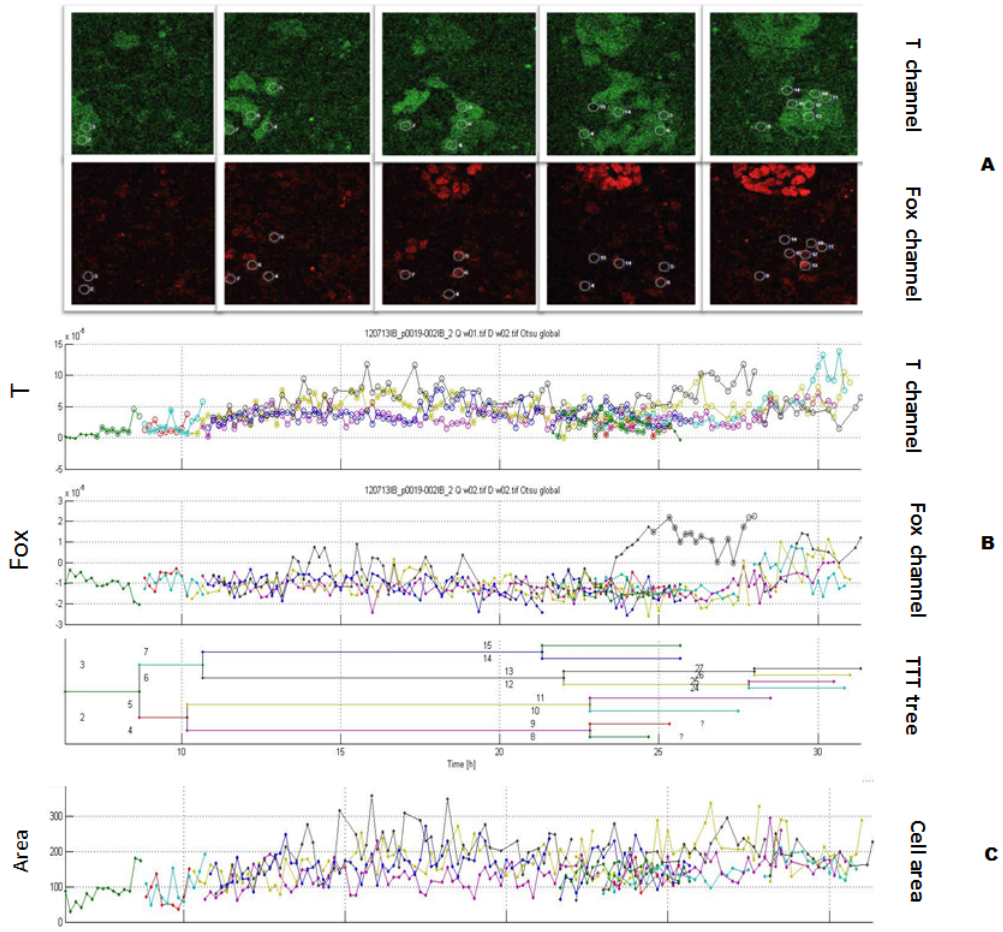

Figure 3.4: Modified QTFy time courses for specific negative gate.
A) image of both channels of several time points.
B) time courses: big unfilled circles represent true signals, small filled circles represent negative signals, big filled circles are representing the change from true to negative signal for two contiguous cells. First row belongs to T expressed cells and second row to Fox expressed cells.
C) Area courses for every single cell at every time point, important for the cell area dependent calculated gate, unusual big cells lead automaticaly to a higher intensity value (see chapter 2).

The display of filled and unfilled circles provides a detailed possibility to recognize which cells are negative or positive, at every measured time point. Unfilled circles are illustrating a signal and filled circles are just background noise. Starting with Fox analysis, the first twelve cells are under the gate, and first signals are detected for cell thirteen, but not as continuous signal. First this seems to be an incorrect way to analyze branches, though a second view shows a quiet different perception. Looking back at the cells of the origin QTFy time course, cell thirteen alternates a little bit and every time when, the peak is increased, the specific negative gate is positive. At the next time point the line decrease and the signal circle is filled. The signal is near the point of being a real Fox differentiation and touches the gate border. The quantification is considered to be accurate as the visual impression leads to very similar results. There is no real signal for Foxa2, a little bit more intensity or perhaps a

different cell size will possibly change this result. In comparison to the two methods above, the specific gate gives also an impression of how near a cell is to the negative gate border. The global gate with background correction is very close to the result with a specific negative gate, but probably this method is sometimes not critical enough and there are too many false positives. In the showing example we would say both, the background corrected global gate and the specific gate, are very accurate methods, but the last one gives more information about the fine line between positive and still negative signals. Here, the simple global gate leads to the same result as the specific gate, but there is no opportunity that the nearby positive cell thirteen may be positive. This gate misses too many signals.

T analysis lead to the same conclusion. The specific gate is something like an intermediate gate of both global gate methods. This can be seen, for example, for cell one. The normal global gate submit that the cell is only positive for the last two or one time points. The extended global gate indicates a signal after the third cell, while for the specific gate the cell slowly turns the marker on and in the middle there is a true signal.

The illustrated tree is just one example of a tree where one of the global gates gives a wrong signal and the other a inaccurate one. Here is also the problem, like before, that the movie is made without an additional nuclear marker, and segmented cells could be wrong. The use of global and individual gates on the other movie is also shown (see 3.1.5.) getting an impression of the nuclear marker influence. Again the T expressed cells are positive in all three methods, certainly the corrected global gate provides a precise gate. For example for cell two, the global gates indicates no real signal for Fox, only for the last two cells. Additionally the specific negative gate (see Fig. 3.5C) also gives arise, if the cells are about to become positive, indicated through a frequent change of expressions, which is then illustrated by big filled circles. Like for the analylzed tree from set 1, the specific gate is an intermediate gate of both global gates. With this gate, it is easy to decide which cells, and then which branches, are positive. Noticeable are the values for background corrected intensities, different from the previously corrected cells (see Fig. 3.4.B), there is only a horizontal shift, which is a result of the H2B-CFP segmentation for both markers.

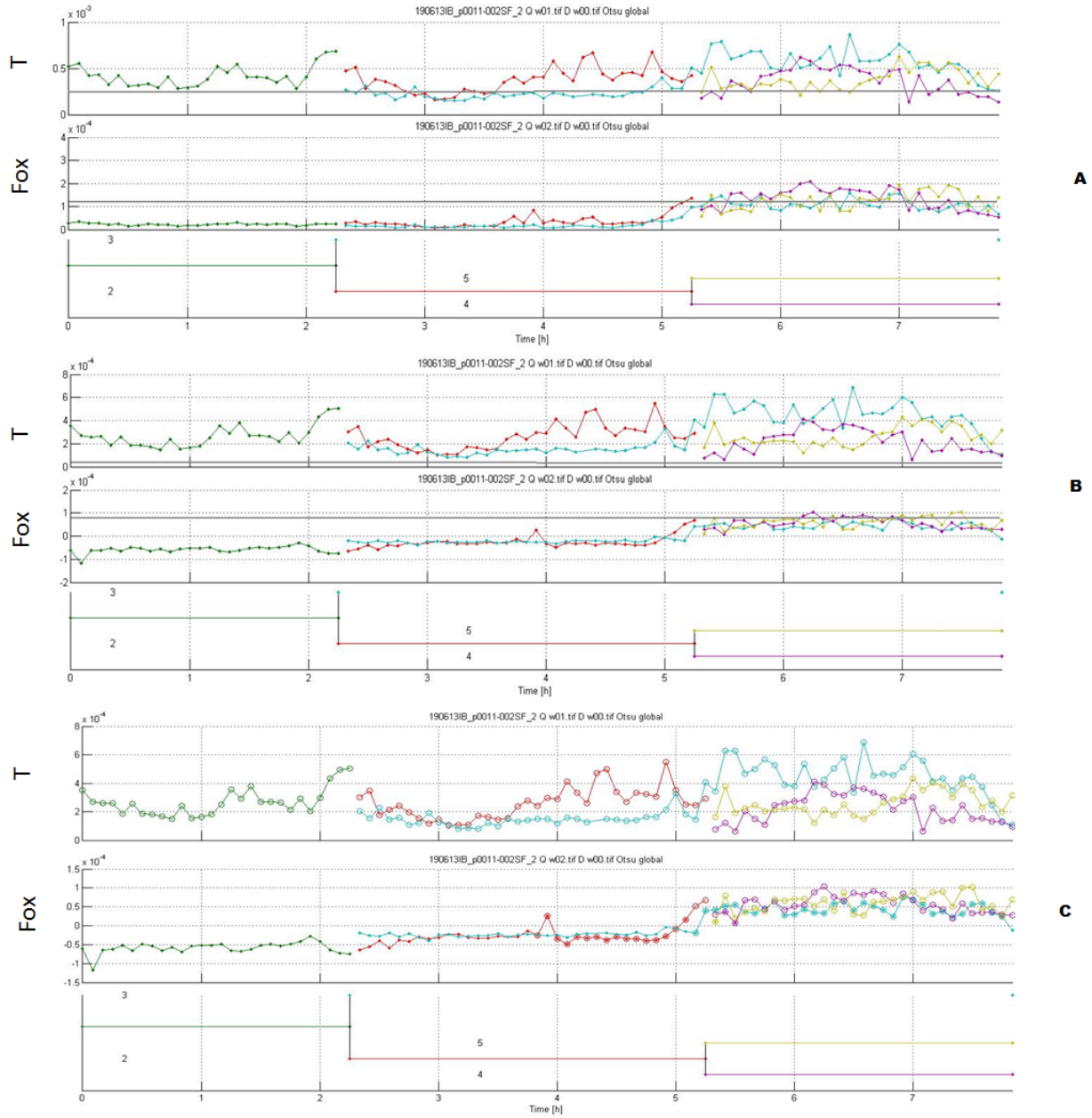

Figure 3.5: Comparison of different gates for an unbiased tracked tree.
Gates were calculated for one tree from set 3 A) Global gate without background correction (T =$2.65 * 10^{-4}$ Fox = $1.32 * 10^{-4}$) B) Global gate with background correction (T = $0.24 * 10^{-4}$Fox = $0.18 * 10^{-4}$), the time courses are background corrected by subtracting the mean background intenstiy for every single cell individually C) Specific negative gate: small filled circles are showing negative cells, big unfilled circles represent positive cells. The big filled circles correspond to a change of positive to negative marker expression consecutively. The time course is also backgroud corrected, like the cells from the global gate with background correction (B).

Analysis for T	Global neg. gate without bc	Global neg. gate with bc	Specfific neg. gate
Positive timepoints	1123 (22.17%)	4180 (82.50%)	3537 (69.80%)
Negative timepoints	3944 (77.83%)	887(17.50%)	1530 (30.20%)

Analysis for Fox	Global neg. gate without bc	Global neg. gate with bc	Specfific neg. gate
Positive timepoints	409 (8.07%)	105 (2.07%)	303 (5.98%)
Negative timepoints	4658 (91.93%)	4962 (97.93%)	4764 (94.02%)

Table 2: Global comparision of different negative gates.
All cells from the unbiased set3 were analyzed with each negative gate method. Tables are showing the distribution of cell numbers for T (Fox) positive expressed cells and T (Fox) negative expressed cells. Numbers in brackets show portion of positive and negative cells, in total 5067 cells were used for this analysis.

By applying the three different methods on every tree from set3, the following conclusions can be made:

Analyses of T and Fox are showing similar results and the global gate without background correction characterizes only a few cells as positive. Especially for T, there is a great difference between the global gate with and without background correction. As assumed before the specific negative gate is in between the two global gates.

3.2 Marker intensity correlation

One main analysis is the influence and possible correlations of the two transcription factor. For this kind of analysis only cells from set3 are used. There is no obvious correlation between the cell intensities form set 1, referable to the inaccurate segmentation. Therefore all intensity values from all tracked cells are illustrated. To be expected is a none-random correlation, because of the assumption of a mesendoderm both factors have to correlate in some way. Which will indicate some predictable patterns and this could be useful for a better understanding of ES cell development.

Frist, the correlation between uncorrected cell intensites is shown (see Fig. 3.6.A). The correlation matrix looks very clear with defined lines. Between Fox and T, a linear correlation can be observed, both intensities increasing simultaneously. This leads to the first assumptions, that there is no meaningful correlation between these two markers. The intensies are dependent on cell size, bigger cells are expressing a stonger intensity for both markers. This is probably one result of the protein content, which is doubled through the cell cycle and with an increase in size the number of proteins are increasing too.

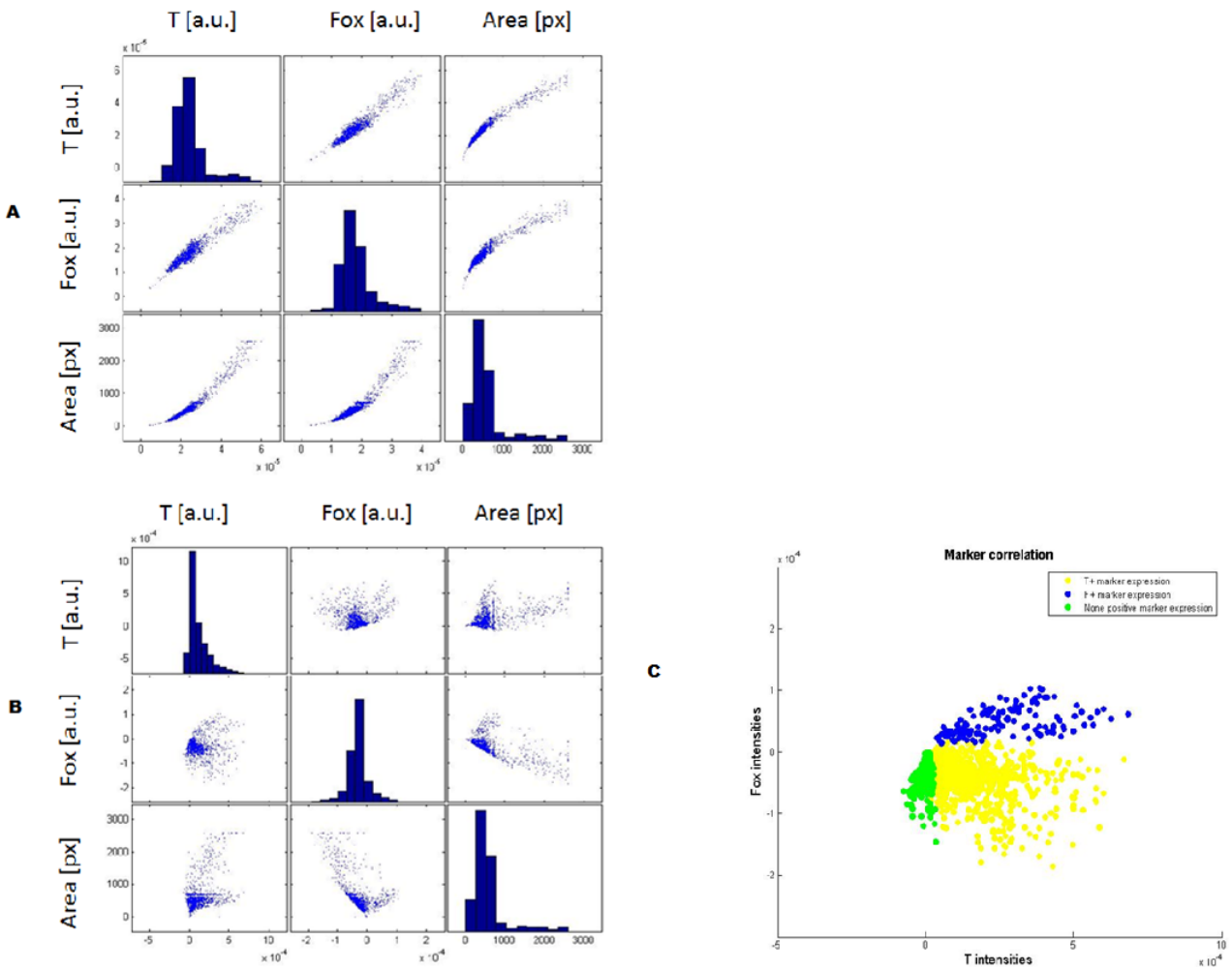

Figure 3.6: Correlation matrix

Correlation matrix for T intensity, Fox intensity and cell area of all measured cell timespoints from set 3 (for detailed information see Table 1).
A) Correlation Matrix for uncorrected cell intensity values.
B) Correlation matriy for corrected cell intensity values.
C) Detailed correlation for Foxa2 and T. Cells expressing a T positive cell signal are illustraed in yellow, Fox positiv cells are purple. Double positive cells are having a blue color and also negative cells are shown in green.

The histograms are showing the distribution of the particular marker or cell size.

The background correceted version of set 3 is more interesting (see Fig. 3.6.B). Like already mentioned, the movie is dominated by positive T expressed cells. This observations are also provided by the shown histograms, intensity values smaller than zero are indicating a negative cell signal. Most of the Foxa2 expression are having zero cell intensity values, only a few cells could possibly be positiv. However, only a few T cell intensites are lower than zero. The correlation between the two markers is shown in detail (see Fig. 3.6.C). As expected, the different positive cell expressions are showing clearly difined cluster. Most of the cells are only positive for the green fluorescent transcription factor. Cells without any positive signals are located in the upper left part of the plot. While double positive cells are only in the upper half.

Again, by comparing the matrices, the need of a background correction is demonstrated. Only for these cells, any correlations are shown and different marker behaviors can be observed. Also the correlation with cell size is more specific, there is not only an increase in cell intensity by increasing the cell size. Most of the cells are having nearby the same cell size with an indpendent increase in cell intensity. Fox intensity decrease while the cell area increase, this is an indicate of negative cell expression, independent from the cell growths, the marker is still negative. Because of this, there is no wrong interpretation of false postive signals, resulted from bigger cells.

3.3 Cell cycle analysis

3.3.1 Lineage and generation specific cell cycle lengths

There are various possibilities to gather new insights with the aid of cell cycle information. One main question arises immediately, if there is any effect due to cell cycle. First we wanted to test, if there is a lineage specific effect of cell cycle length. One possibility is to apply an analysis of variance test, anova test, to compare the variance between the trees with the variance within each tree. Therefor the cell cycle lengths of all trees are compared, but it is not possible to use every tracked cell. The first cell is always removed, because there is no clear starting point of the cycle. Also the last cells are removed, because there is no clear ending point of the cycle. Starting with set1 the first surprisingly observation of the remaining cycle lengths are noticed, some cycle are too short to be a biological real process. In such a short time the mouse mitosis, the process of cell division, is not able to run through all indispensable stages, like the spindle apparatus formation.

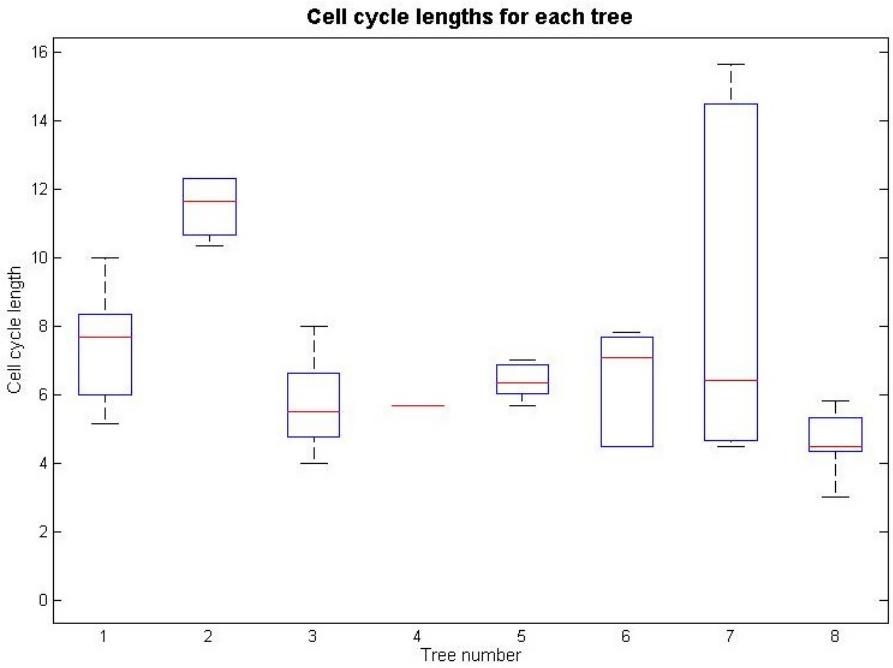

Figure 3.7: Cell cycle lengths of tracked trees.
One box represents one tree, including several cells. No lineage specific effect can be seen by comparing the mean values (red lines) to each other, if the mean cycle length is about the same for every tree, the assumption of a lineage specific effect is accepted. The average should also be in the middle of the box, which indicates a uniformly distributed distribution.

By looking at the movie, and thereby at the critical cells, we determine all of these trackings are based on only T expressed cells. Sometimes the cell boundaries are not clear and it is not possible to classify one cell in a cell colony, so it is also difficult to see a division. Such short cell cycles are caused of a tracking mistake. All of these short-division cells were tracked wrong and we have to remove them to get an imposing result. The remaining cycle lengths are used for the anova test. Of eight different trees, also tracked from different positions, the durations until one cell divides is calculated and used for this analysis. The resulting p-value, the probability of obtaining a test statistic, is calculated and the hypothesis of a significant correlation between the cycle lengths is reject, if the value is bigger than 0.05 or accepted if the value is 0.05 or lower. The computed significance value, $p = 0.055$, indicates a rejection of the hypothesis and leads to the result that there are no similar cell cycle lengths and so no lineage specific cell cycle effect exists. By looking at the mean length within a tree (see Fig. 3.7) not even these are having a common lengths. And for the comparison between the trees it is obviously that there is no correlation. For example, tree 7 compared to tree 8: the mean value is 8.69 hours against 4.58 hours, a cell division need half (double) of the time. But there are also great differences in degree of deviation, tree 7 has a standard deviation of 5.03, which indicates a none similar cycle lengths within this tree. Probably some other cells are having the same cycle time like, for example, cells from tree 6.

There are also problems by applying the anova test on set 3, based on far too little cell

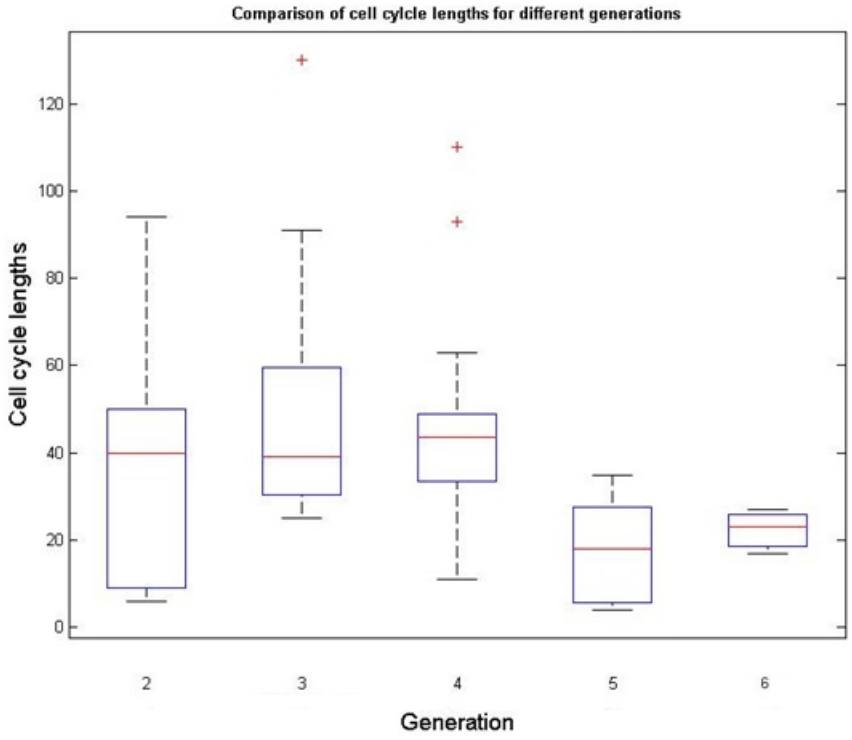

Figure 3.8: Cell cycle lengths of different generations.
One box represents one generation, including several trees. A generation specific effect can be seen by comparing the mean values (red lines), if the mean cycle length is nearby the same for every tree, the assumption of a generation specific effect is rejected. The mean should also be in the middle of the box, which indicates an uniformly distribution. The red crosses are illustrating values which vary tremendously to the rest.

divisions only a few lengths can be used for the statistical test. Because of this, the result is not representative but there is also an advantage of this set, the additional nuclear marker. With this marker the tracking is more accurate and no short cell cycles, like in set1, are contained in this and set so every tracked cell division is useful. The hypothesis is also rejected ($p = 0.45$), there is also no correlation between the cell cycle lengths.

As shown before, there is no correlation between single trees.This begs the question, if there is eventually a generation dependent cell cycle effect. Therefor the cycle lengths are sorted by generation (see Fig. 3.8) and an anova test is applied, again. Altogether there are five generations, already including the removed first generation and also the last generations. On average the duration, until one cells divides is the same for generation three and four (about 8 hours), while the cycle lengths of the last two generations is too short to be a real biological cycle (around 3 hours). But not only the mean value also the standard deviation should be mentioned. Especially for the first generation there is a

high tendency towards shorter cycle lengths. The resulted p-value from the statistical anova test provides a significant p-value, p=0.016, and out of this there seems to be a correlation between generations. Again it is clearly recognisable, that the cycle lengths are too short to be a real biological cell cycle, which is caused by the previously explained problem.

3.3.2 Cell cycle dependence of T and Foxa2

Another interesting concept is a potential correlation between intensities and the cell cycle length. Therefore both sets are observed, set1 offers the problem of possible wrong tracked cells, but is worth consideration. set2 is not representative because of too little branches. For intensity the mean value of all signal values during the cycle length is used. There is also the possibility to use the median of the first three values, but this is not shown here.

Starting with set1, looking at T intensity versus cell cycle length, two distinct clusters emerge (see Fig. 3.9.A). The first cluster containing low intensity values (0.00008 - 0.000015) with a cell cycle time ranging from 4 to 14 hours. Cluster two seems to have higher intensity values for a shorter cell cycle lengths, only between 4 and 8 hours. Also a pearson correlation coefficient (corr) is calculated to get an impression of the correlation between marker intensities and cell cycle lengths. If the value is bigger than 0.005 the hypothesis of an correlation is rejected and otherwise there is a correlation. In this case corr=0.08 and the hypothesis is rejected, there is no correlation between T expressed intensities and the corresponding cell cycle lengths. Noticeable is the presence of two obvious cluster, one possible explanation for them are the tracking problems based on single positive T expressed cells, like explained previously.

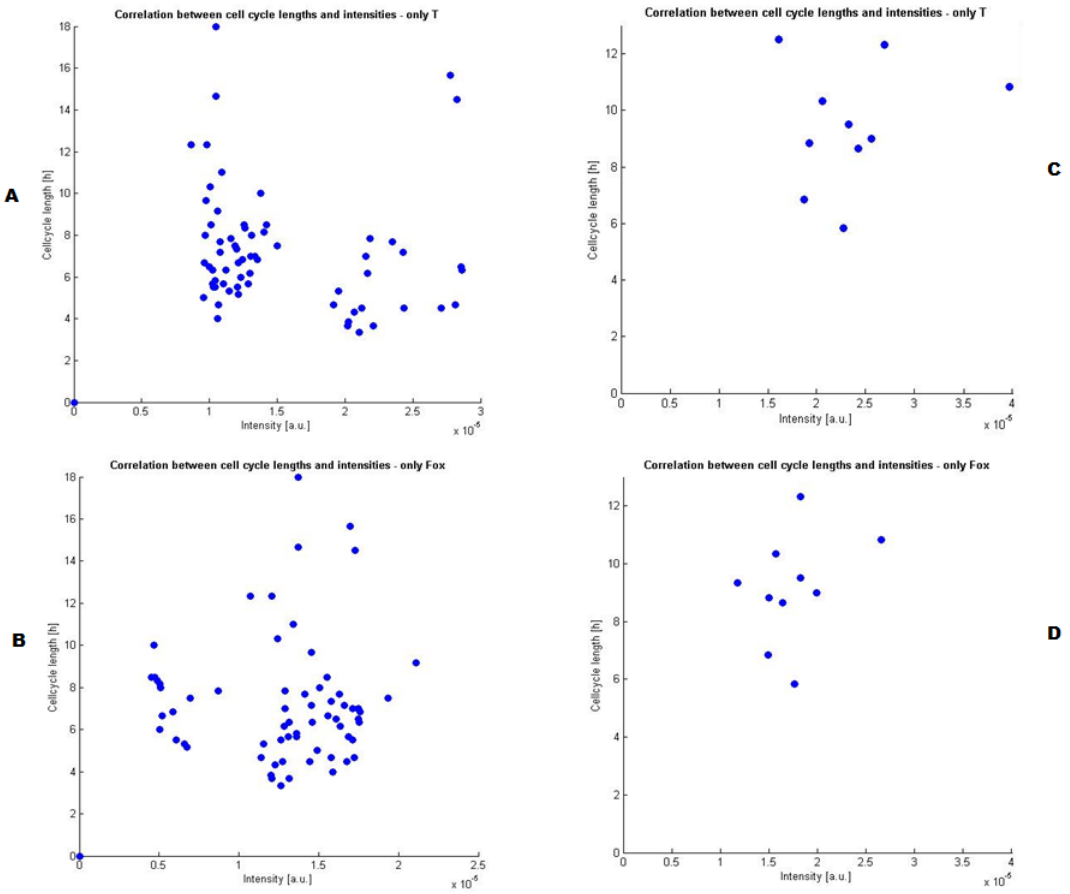

Figure 3.9: Correlation between marker intensity and cell cycle length.
First scatter plots (A and C) are showing the intensities for brachyury expression and the second (B and D) for Foxa2 expression . For the plottet intensities the mean intensity value of a cell cycle is used. Important facts are caluclated for every single plot: mean +- (standard deviation) and the pearson correlation coefficient (corr).
Pots based on set 1 :
A) For T intensity against cell cycle lengths : $1.89 * 10^{-6} + -5.44 * 10^{-6}$ **and** $corr = -8.78 * 10^{-2}$
B) For Fox intensity against cell cycle lengths: $1.60 * 10^{-6} + -4.50 * 10^{-6}$ **and** $corr = -4.24 * 10^{-3}$
Plots based on set 3
C) For T intensity against cell cycle lengths : $2.37 * 10^{-5} + 6.53 * 10^{-6}$ **and** $corr = -1.15 * 10^{-2}$
D) For Fox intensity against cell cycle lengths: $1.74 * 10^{-5} + -3.94 * 10^{-6}$ **and** $corr = 1.19 * 10^{-1}$

For the next analyze the Fox expressed value are compared to cell cycle lengths (see Fig. 3.9.B), the plotted values can be separated into two cluster, again. The first cluster is smaller than the second one and contains just low intensity values (0.000004 -0.00001), compared to the low intensity cluster from T, the values are about one-tenth lower and the cell cycle lengths are only between 5 to 10 hours and also shorter than for the other marker. The second cluster seems to have higher intensities, ranging from 0.00001-0.00002 and the maximal cell cycle length is around 16 hours (min. 3 hours). Interesting is the pearson coefficient (corr = 0.0042) which indicates a correlation between the variables. The correlation is resulted from better tracking conditions, with the nuclear Foxa2 marker.

R - square	0,034910989
Adjusted R - square	0,003268726
Observations	64

	beta - correlation coefficient	standard error	p - value
Cell cycle lengths	8,810530684	1,382955015	-
T marker expression	-92723,57617	64381,15194	0,154915699
Fox marker expression	-8172,296572	87471,74965	0,925869865

Table 3: Regression table and detailed summary.
First table : short overview about calculated $R^2$and how many data points are used for the linear multiple regression.
Second table : multiple regression output; beta, the correlation coefficient, for directed (first row) and undirected values (second and third row), standard error and p value should be as small as possible. If they are small enough (p <0.005) then a significant correlation between the undirected concerning to the directed variable is taking place.

Testing the same with cells from set3 (only a few cells were used see previously explanation) a more accurate result is expected, already at a first glance the cell cycle lengths are long enough to represent a real cell division (see Fig. 3.9.C, D). The cycle lengths for both transcription factors are about the same and it seems to be higher intensity values for T expressed cells than for Fox expressed ones. By comparing the correlation an interesting observation can be made, as distinguished from the results from set1, the correlation for fluorescence markers is the other way around, it seems to be a correlation between cell cycle length and T expression (corr = 0.001) and no correlation for Fox (corr = 0.11). No deceleration can be made about the correlation of one marker and the corresponding cell cycle length, further analysis are needed.

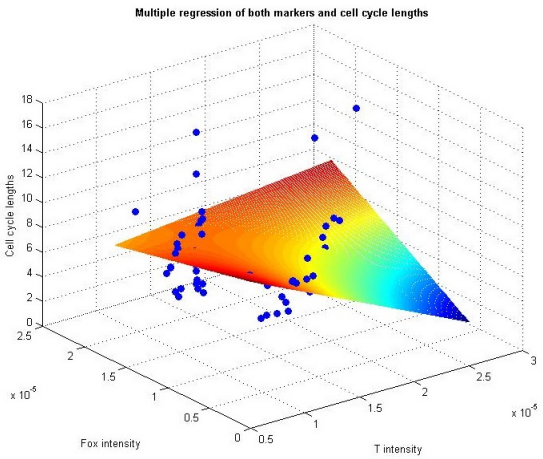

Figure 3.10: Illustration of multiple regression results.
Linear multiple regression used on set 1: x-axis contains all mean intensity values for Fox, y - axis contains all mean intensities for T and z - axis shows different cell cycle lengths. The plain should cover all points, to fit the data for getting an impression of the correlation.

With the help of a linear multiple regression, an even better comparison of the functional interaction of all parts can be seen. The regression coefficient, beta, is the standardization of dependent and independent variables. In this case, the independent variables are T-intensities and Foxa2-intensities and the dependent variable is the cell cycle length. First we made the multiple regression test on set1.

Analysis shows a very low $R^2 = 0.03$, which only indicates 3% correlation, and the adjusted R square is also only around 3%. There is a low p-value for T, which is evidence of significance, but for Fox, the values goes towards one (see Table 2) and so not significant.

The extreme high and low regressions coefficients lead to the assumptions, that there is a multicollinearity a problem when two independent variables are highly correlated and so the estimation method becomes instable. The attempt to find a regression plain does not work very well. It is not possible to put a plain through all points.

By taking the same steps for set3, at least the same plain is expected. The illustration (see Fig. 3.10) is not insightful, because of the less applied points, and also R^2 is still too low. Above all the adjusted value is only 15%, which leads to the conclusion that there is no proportion of the variation in the dependent variables, which could be explained by variations in the independent variations. The worth beta value is the same like for set1. The difference is that one number is highly positive and the other is negative. The comparison of both plains does not lead to obvious results.

3.3.3 Intensity values of normalized cell cycle lengths

The cycle lengths were normalized to get a better impression of expressed intensity values with an increase in lengths.

For a better illustration, only trees with enough cells from set3 are used. With too many cells (like in set 1) the plot will not be easy to analyze. Therefore an averaged intensity for all cells of every cell cycle length percent is a better way to illustrate the correlation (see Fig. 3.11.). To get the intensity value for every percent of cell cycle length, the mean value is calculated and plotted for every intensity value (see Fig. 3.12.). For both transcription factors, the pattern looks similar. For most cells the mean intensity stays around the same level independent from the cell cycle progress. Only sometimes at the beginning a small fluctuate can be observed. The mean value will be stabilized at a specific intensity value.

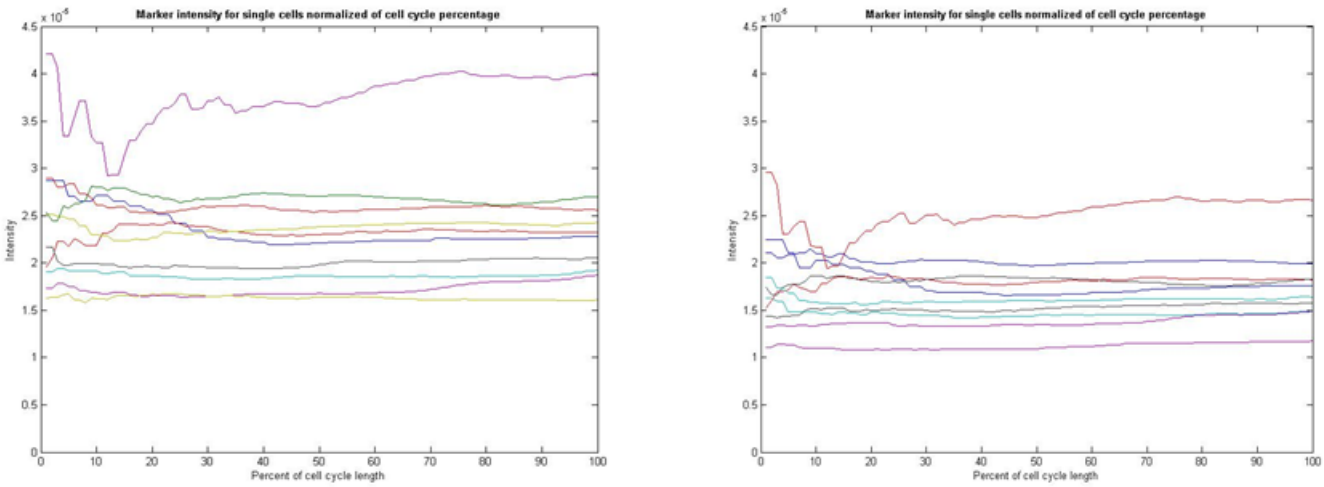

Figure 3.11: Normalized cell cycle length for mean intensity values.
Lines representing one tracked cell of the unbiased set, for every percent the mean intensity value of the actual cell cycle length is calculated.
Left plot : normalized cell cycle length for T intensity values.
Right plot: normalized cell cycle length for Fox intensity values.

The only difference between the two markers is a shift along the normalized cell cycle lenghts, for T more into the positive area and for Fox these lines are between 0.00001 and 0.00025. Just one cell deviates from the rest with a strong fluctuations at the first 30%-40% of cycle lenghts. Interesting here is the notable high intensity values. To figure out if this large difference is real, it is necessary to look again at the tracked ttree. The curvy line at the beginning results from dead cells, which are passing through the movie and lay over the traced cell. The extreme high values are probably because of the double positive cell (the line for Fox cells is also therefore different). No exception can be observed while watching the movie for this cell, there are no other conditions while making this position, the light is the same like for the others and there are no differences in background noise. By comparison to cells from set1 (see Fig. 3.11.) the mean intensity value is almost the same for every cell, which means for T expression around 0.000012 and for Fox around 0.000013. The standard deviation for Fox expressed cells is lower than for T, which referable to the cytoplasmatic green fluorescence marker.

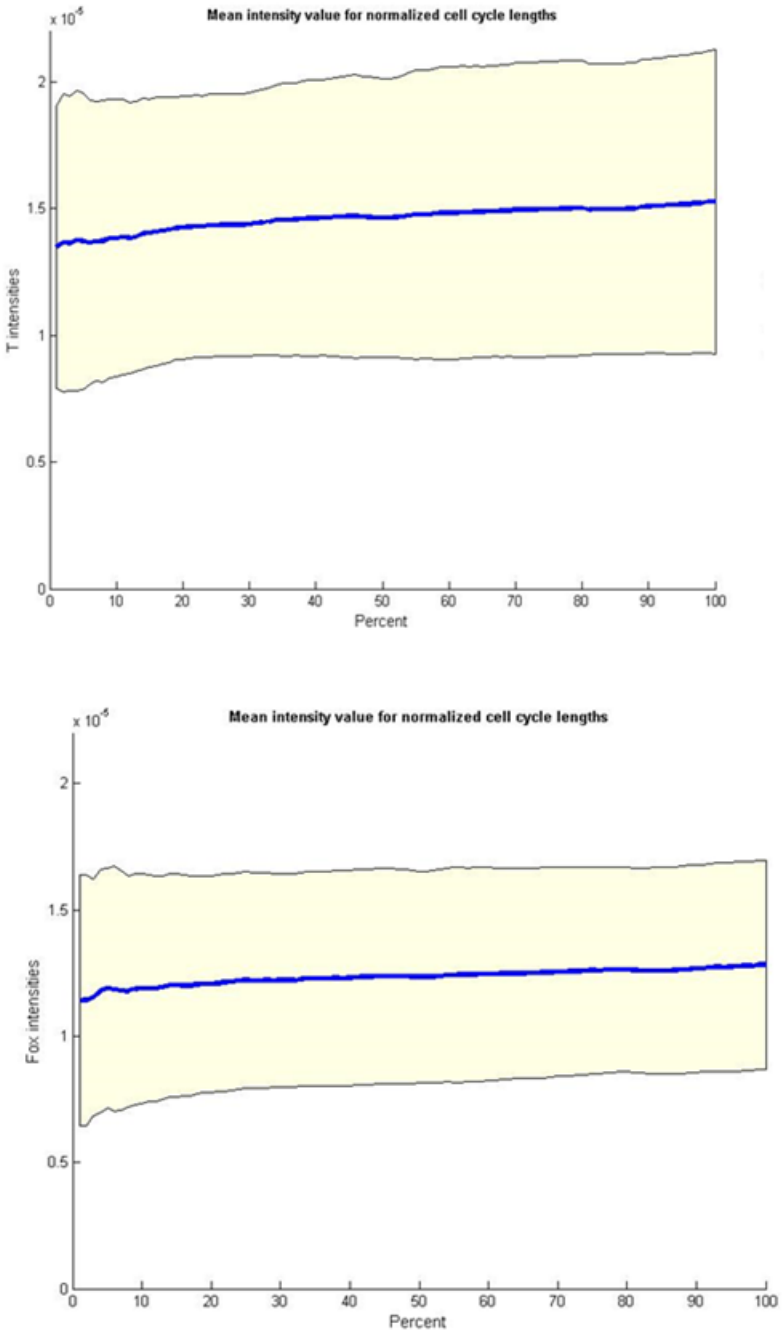

Figure 3.12: Intensity value for normalized cell cycle length

Normalized cell cycle lengths against marker intensity: The mean intensity value (blue line) for all cells, from every tree, for a particular percent value is calculated. Having a lot of cells (72 cells) it is also important to give advice about the standard deviation (yellow shaded area) for each percent.

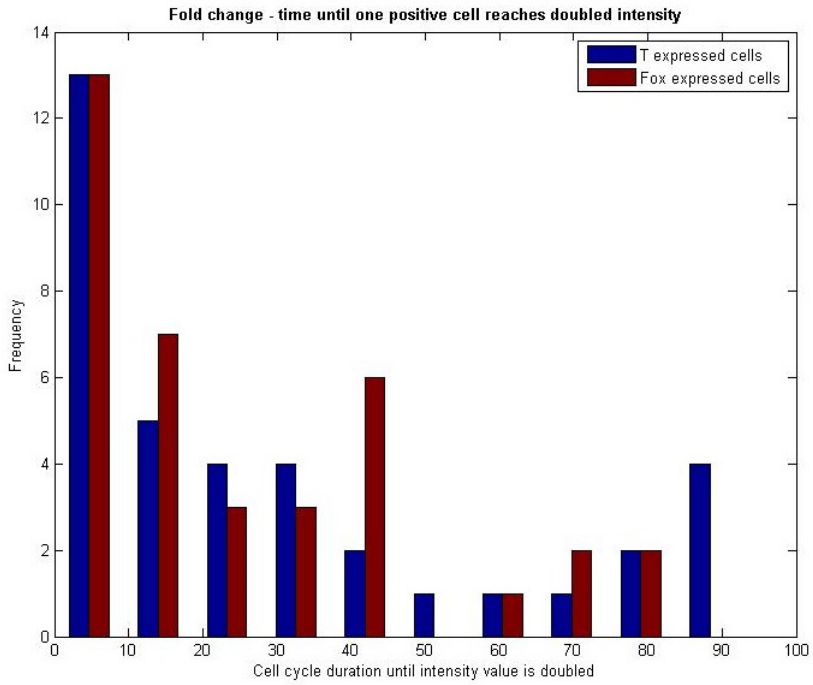

Figure 3.13: Duration in time points until one positive cell doubled its intensity. **There a two different bars which are corresponding to the T expressed cells (blue) and Fox expressed cells (red). The plot is showing the duration until one positive cell doubled its protein intensity applied to all cells from set 3. Cells which are not doubling its content during one cell cycle, the time point until one daughter cells gets the doubled value are used, for this analysis.**

As a last statistic the fold change of differentiated cells s analyzed. This means the time one cell needs to double its protein content. For that analysis the protein intensity of the first positive classified cell is chosen. Then the the time until the cells reaches ists doubled intensity value is measured.

If one cell does not reache its doubled value until one cell cycle, the intensity values for both daughter cells were used and the duration until one of this doubled the mother-cell intensity value is measured. Almost every cell reachs its doubled intensity by the first ten time points (see Fig. 3.13.), indepent of T or Fox. For a few T cells, the cycle length is between 10-30 time points.

Five cells have a cycle length of around 90, which means the cell needs 90 time points (15 hours) to double its value. Remember the results came from set 3, an unbiased set where all cells are tracked, and some cells without divisions were also analyzed. These few cells belong to none-dividing cells.

A slight difference can be observed for Foxa2 expressed cells. Altogether the cycle is longer (excluding the T none-dividing cells) and on average a cell needs 32 time points (5.3 hours) for doubling its intensity value, whereas T takes nearly five hours. A tendency towards one specific duration is shown, but no obvious marker specific cell cycle length.

3.4 Differentiation pattern

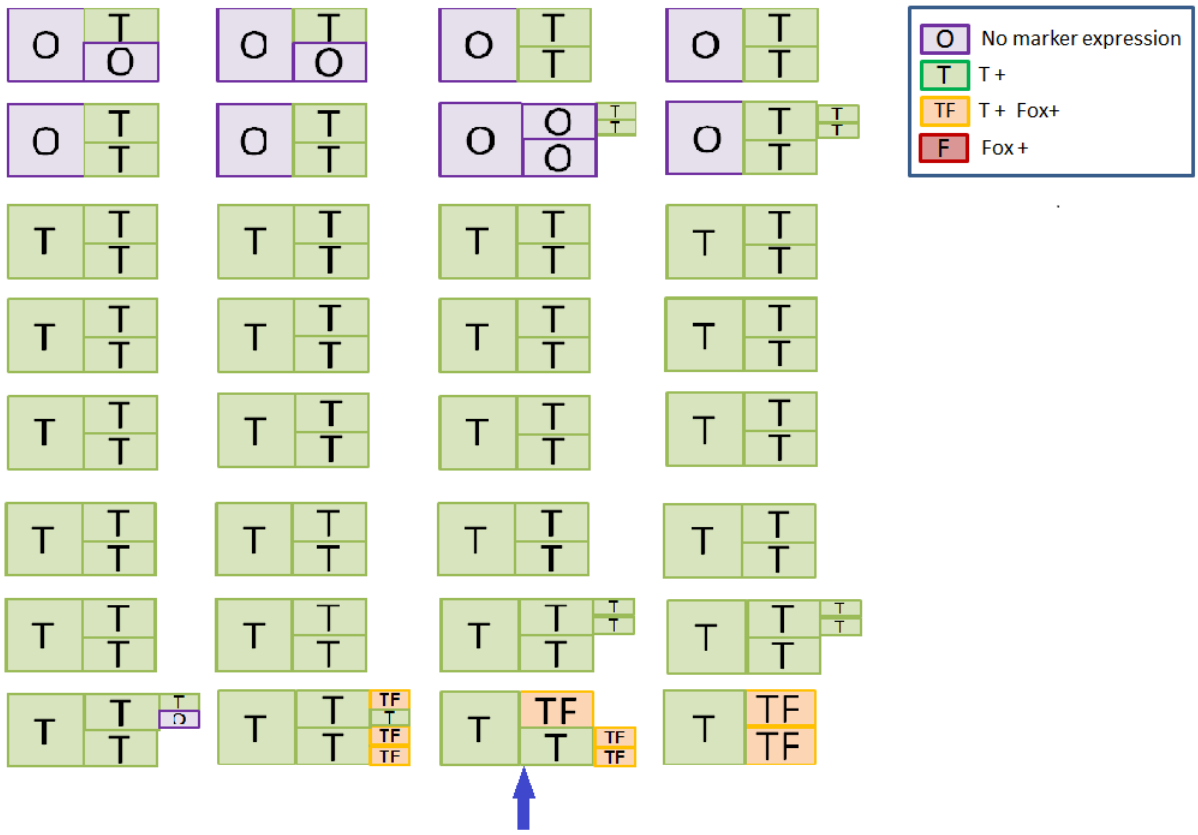

Figure 3.14: Pattern of marker expression for every single branch in one tree.
Pattern of trees from set 3 (excluding all none-dividing cells): One branch is expressing a real positive signal, if there are more than eight consecutive cells over the specific negative gate for one (both) markers.
Green boxes = positive T expressed; orange boxes = double positive branch; purple boxes = no differentiated cells; red boxes = positive Fox expressed branch.
To find one, out of the three possibilities, the conditions for the last few time points are detected and used. Sometimes the positive and negative cell expressions are fluctuating; therefore the more stable looing one is used. The blue arrow marks an interesting pattern, which is different than the others. Trees with no divisions are only expressing the transcription factor T.

In the last section of the results, we analyzed the expression of both transcription factors for one branch to get a better impression of expressed patterns. For every tree of the unbiased set3, a branch-specific pattern is illustrated (see Fig. 3.14.). With this illustration it is easy to see all possible patterns of differentiation combination. Most of all T is expressed at the beginning, and also the two daughter cells are positive expressing T. Only sometimes another model is observed. It is also possible, that after a division, a T positive cell divides into two or one double positive cell. Unexpectedly there is no cell expressing only Fox- and the mesoderm transcription factor T is always turned on before Fox is starting its expression.

For sure the movies are too short to give an accurate result, but a lot of cells do not pass the mesendoderm step and are double positive before deciding to be endoderm or mesoderm.

Interestingly there are trees which divide into two different types. For example: one cells is T positive and after dividing, one daughter cell is double positive and the other single T positive (see Fig. 3.14. blue marked pattern). Later the single positive cell divides and then two daughters themselves are double positive. This brings the result of a time-displaced marker expression, one marker turns on for one cell and the other needs more time, probably like in this case another division, to get the same marker expression.

The set is an unbiased tracked tree set, but surprisingly for all cells T is always expressed. When starting tracking only a few cells are having no positive signal. But they also become positive after a few hours. Unfortunately, patterns from set1 are too vague to make the same illustrations. It would be interesting if a movie, having a lot of cell divisions like in set3 and including the easy tracking nuclear maker, as in set1, would show the same patterns.

To go a little bit more into detail the expressed cells for each time point are evaluated. Therefore the whole unbiased set (including none-dividing cells) are used to get an impression of expression ratio. Like already seen in the figure before, most of cells are T-expressed (see Fig. 3.15.). There are also a few cells which are only Fox positive, but these are too little to see it on the figure. Towards the end the total number of cells become smaller as a result of prematurely end of tracking. Cells which were tracked until the end are always only expressing T. By calculating the ratio of all possibilities over 70% of all cells express T, until the 130 measurements, and only 5% are double positive cells. There is also a decrease in double positive cells, the small number from the start is even smaller while the number of time points increase.

It is also possible to give an statemant about the average delay by looking at the time span between T and Fox. Therefore it is important, that T does not have a positive expressing at the first time point. Only for one cell Fox is getting a positive expression and T is negative at the beginning. The duration until the cell becomes double positive takes 13 hours. Because of this it is not possible so derive any results.

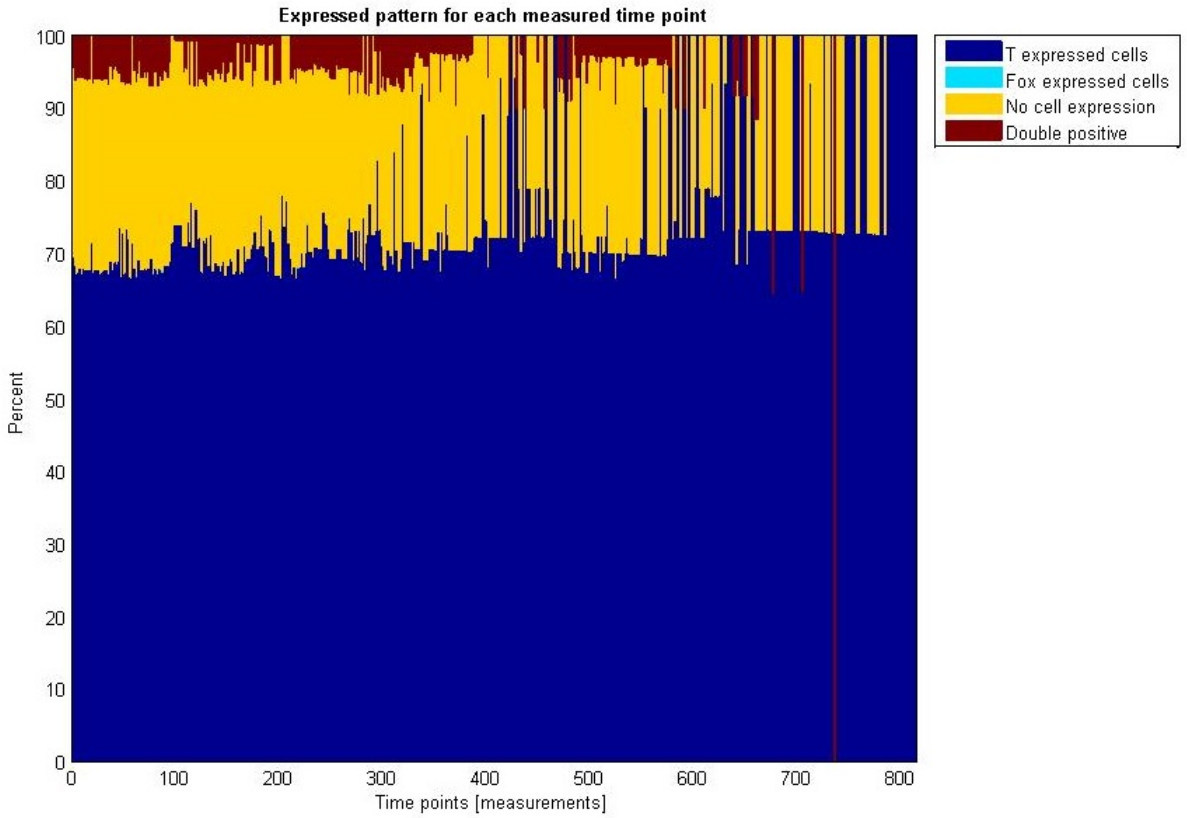

Figure 3.15: Normalized marker expression

Percentage of expressed marker for every measured time point, sorted by cell number. Fox expression is too low to see it in the figure.

To not only show not only the expression of independent single cells, also the spatial distribution was analyzed at several time points (see Fig. 3.16). Cells are again separated into the four previously introduced properties.

Starting after five hours, three separate colonies are clearly recognizable. From then on a greater part of the cells have already acquired a positive T expression and only are few cells which are negative for T as well as for Foxa2. Surprisingly two cells already are double positive.

After ten hours most of the negative cells turned into T positive cells. The two classified double positive cells, identified at the five hour time point, are apparently not real. Probably these cells were positive only for a short time and no real Fox expression can be derived. Certainly there are two different double positive cells at this time point. It can be observed that cells, which are either expressing T or Fox, are located at the edge of a colony.

Finally the physical configurations of cell colonies are regarded towards the end of the movie are. Additionally certain cells turned on Fox, so more double positive cells can be observed. These are rather located along the edge. At that moment only a few cells are negative.

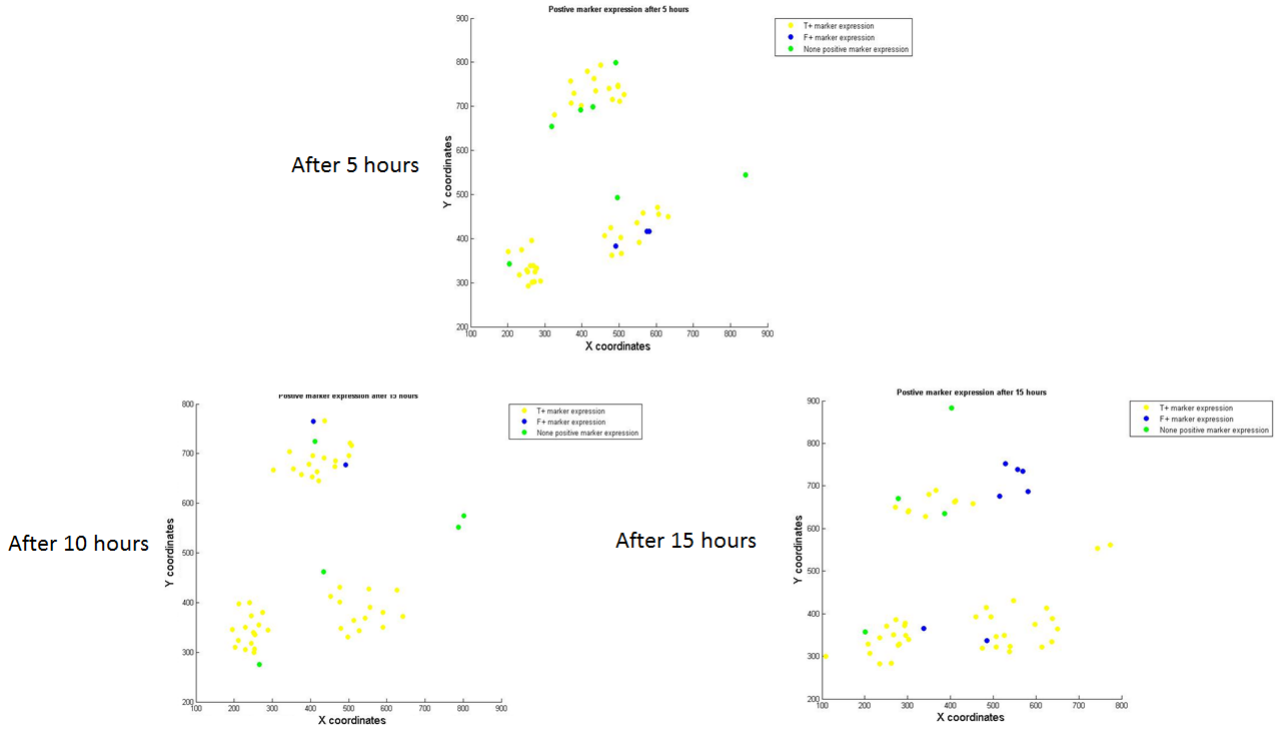

Figure 3.16: Spatial distribution of cell colonies after several time points.
Spatial distribution of cell colonies, cells are labed based on its positive marker expression. Different colors illustrate the four possibilities: Cells having a positive T signal (yellow), cells having a positive Fox signal (gray), double positive cells (blue) and also these one without any signal are shown (green). The development of cell colonies is shown, in a five hour intervall.

4 Discussion & Outlook

In the beginning of this project we asked whether there is a mesendoderm, and when and how long the fluorescent markers (T-GFP and Foxa2-TagRFP) are having a positive expression. After several analysis and different evaluating steps, it can be said that there is some correlation between the expression of both markers. There is no significant correlation between cell cycle length and marker expression. During the analysis we got the idea of a third nuclear marker for better cell tracking, a better quantification and analysis. With this new marker, a was able to track a unbiased set individual patterns were found with real background corrected signals. But this unbiased set, is too small and only includes one position with just a few time points, comprising 15 hours, and it is not clear if the really low expression of the second, Foxa2, channel is real or just a technical problem. Therefore, more data sets, with more positions, running for two days is needed to repeat all statistical observations and likely find different results or confirm the actual results. As soon as the dataset increases and consequently more different patterns are possible, tree pattern analysis can be applied. To mine such patterns, an algorithm was implemented by Bernd Streppel [35] and can be also applied on these kind of movies.

During this study, it was the first time that someone used the quantification tool QTFy and analysis the question with the mesendoderm on the single cell basis.

Definitely one main result has been established: a method, that calculates for every single cell a revise intensity value, is necessary and an essential condition for further evaluations. The background correction has to be made for every single cell individually. But after these correction But after these correction intensity values that exceed the background value can be identified and are not a result from technical background noises or other no biological influences.

For all three tracked sets, T is the transcription factor which always turns on first. In some cases after a few hours, Fox turns on also, but this event did not take place every time. So it is possible that some cells only express T even after many divisions. In most cases, cells quantified only by tracking without accurate segmentation with QTFy having only a Foxa2 expression are wrong quantification. Background noises for this channel seems to be stronger than they really are. Perhaps the nuclear marker and the strong and intensive red fluorescence marker lead to wrong conclusions. Before using QTFy, I found many trees (from set 1) which only express Foxa2. This would be one great step of rejection of the hypothesis of a mesendoderm. But while treating every single cell, the quantification tool produces another assumption. However, in my opinion, some of these cells expressing Fox result from the again poorly detectable cytoplasmatic T-marker, which often contains too many pixel. The cells are too big, which leads to more intensity values which are summed up, and so a higher intensity value is reached, whereas fewer single Fox-pixels are summed up to the expressed cell value.

First steps towards finding out more about ES-cells are made, but it is a long way to figure out real, biological relevant and substantial results. After this analysis, based on these sets, it is not possible to give a statement about the presence of a mesendoderm and when which factors are expressed exactly.

The next steps will be making new movies over a long time, including many differentiations and especially with the new introduced cyan fluorescence protein marker, H2B. Having such

a movie, all analysis can be repeated on this new set. Another opportunity is to label only a few cells with the transcription factor binding marker, thus the problem with superimposed growing cells is solved. Another important and really interesting analysis will be the cell space within a colony. Therefore the confocal imaging is the best option to gather the volume of every cell in one colony. This topic was not discussed in this work, therefore further extensive analysis are necessary.

If the analysis brings us to the same, or similar, results we bank on these. I am looking forward to get some new movies and applies the new methods and figure out more about this topic.

References

[1] K. Amour, A. Agulnick, S. Eliazer, O.G. Kelly, E. Kroon, and E. Baetge. Efficient differentiation of human embryonic stem cells to definitive endoderm. *Nature Biotechnology*, 23:1534 – 1541, 2005.

[2] SL. Ang, A. Wierda, D. Wong, KA. Stevens, S. Cascio, J. Rossant, and KS. Zaret. The formation and maintenance of the defi nitive endoderm lineage in the mouse: involvement of hnf3/forkhead proteins. *Development*, 119:1301–1315, 1993.

[3] RS. Beddington. Induction of a second neural axis by the mouse node. *Development*, 120:613–620, 1994.

[4] RS. Beddington and EJ. Robertson. Anterior patterning in mouse. *Trends in Genetics*, 14:277–284, 1998.

[5] SP. Beddington and J. Robertson. Axis development and early asymmetry in mammals. *Cell*, 96:195–209, 1990.

[6] M. Blum, SJ. Gaunt, Kw. Cho, H. Steinbeisser, B. Blumberg, D. Bittner, and EM. De Robertis. Gastrulation in the mouse: the role of the homeobox gene goosecoid. *Cell*, 26:1097–1106, 1992.

[7] I. Burtscher, W. Barkey, and H. Lickert. Foxa2-venus fusion reporter mouse line allows live-cell analysis of endoderm-derived organ formation. *Genesis*, 46:512–22, 2013.

[8] I. Burtscher, W. Barkey, M. Schwarzfischer, F.J. Theis, and H. Lickert. The sox17-mcherry fusion mouse line allows visualization of endoderm and vascular endothelial development. *Genesis*, 50:496–505, 2012.

[9] I. Burtscher and H. Lickert. Foxa2 regulates polarity and epithelialization in the endoderm germ layer of the mouse embryo. *Development*, 136:1029–1038., 2009.

[10] M. Cockell, D. Stolarczyk, S. Frutiger, GJ. Hughes, O. Hagenbüchle, and PK. Wellauer. Binding sites for hepatocyte nuclear factor 3 beta or 3 gamma and pancreas transcription factor 1 are required for effi cient expression of the gene encoding pancreatic alpha-amylase. *Mol Cell Biol*, 15:1933–1941, 1995.

[11] Lurich Drews. *Color Atlas of Embryology*. Thieme Verlag, George, 1996.

[12] HM. Eilken, SI. Nishikawa, and T. Schroeder. Continuous single-cell imaging of blood generation from haemogenic endothelium. *Nature*, 457:896–900, 2009.

[13] H.J. Fehling, G. Lacaud, A. Kubo, M. Kennedy, S. Robertson, G. Keller, and V. Kouskoff. Tracking mesoderm induction and its specification to the hemangioblast during embryonic stem cell differentiation. *Development*, 130:4217–4227, 2003.

[14] Scott F. Gilbert. *Developmental Biology*. Palgrave Macmillan: 10th edition, 2000.

[15] H . Grunenberg. Genetical studies on the skeleton of the mouse. xxiii. the development of brachyury and anury. *J Embryol Exp Morphol*, 6:424–443, 1958.

[16] C. Hitz, W. Wurst, and R. Kuhn. Conditional brainspecific knockdown of mapk using cre/loxp regulated rna interference. *Nucleic Acids Research*, 35:527–532, 2007.

[17] JR. Keller, M. Ortiz, and FW. Ruscetti. Steel factor (c-kit ligand) promotes the survival of hematopoietic stem/progenitor cells in the absence of cell division. *Blood*, 86:1757–1764, 1996.

[18] C. Kimura-Yoshida, E. Tian, H. Nakano, S. Amazaki, K. Shimokawa, J. Rossant, S. Aizawa, and I. Matsuo. Crucial roles of foxa2 in mouse anterior-posterior axis polarization via regulation of anterior visceral endodermspecific genes. *Proc Natl Acad Sci U S A*, 104:5919–5924, 2007.

[19] S. J. Kinder, T. E. Tsang, M. Wakamiya, H. Sasaki, R.R. Behringer, A. Nagy, and P. P. L. Tam. The organizer of the mouse gastrula is composed of a dynamic population of progenitor cells for the axial mesoderm. *Development*, 128:3623–3634, 2001.

[20] SJ. Kinder, TE. Tsang, M. Wakamiya, H. Sasaki, RR. Behringer, A. Nagy, and PP.Tam. The organizer of the mouse gastrula is composed of a dynamic population of progenitor cells for the axial mesoderm. *Development*, 128:3623–3634, 2001.

[21] K.Kelland. Scientists create human liver from stem cells. *Reuters*, 2013.

[22] V. Korzh and D. Grunwald. Nadine dobrovolskaïa-zavadskaïa and the dawn of developmental genetics. *Bioessays*, 23:365–371, 2001.

[23] P. Krupinski, V. Chickarmane, and C. Peterson C. Simulating the mammalian blastocyst–molecular and mechanical interactions pattern the embryo. *PLoS Comput Biol*, 7, 2011.

[24] P. Krupinski, V. Chickarmane, and C. Peterson. Simulating the mammalian blastocyst - molecular and mechanical interactions pattern the embryo. *PLoS Comput Biol*, 7, 2011.

[25] E. Lai, VR. Prezioso, WF. Tao, WS. Chen, and JE. Jr. Darnell. Hepatocyte nuclear factor 3 alpha belongs to a gene family in mammals that is homologous to the drosophila homeotic gene fork head. *Genes Development*, 5:416–427, 1991.

[26] Cs. Lee, NJ. Sund, MZ. Vatamaniuk, FM. Matschinsky, DA. Stoffers, and KH. Kaestner. Foxa2 controls pdx1 gene expression in pancreatic beta-cells in vivo. *Diabetes*, 51:2546–2551, 2002.

[27] GR. Martin. Isolation of a pluripotent cell line from early mouse embryos cultured in medium conditioned by teratocarcinoma stem cells. *Proc Natl Acad Sci U S A*, 78:634–7638, 1981.

[28] RJ. Mason, MC. Williams, HL. Moses, S. Mohla, and MA. Berberich. Stem cells in lung development, disease, and therapy. *Am J Respir Cell Mol Biol*, 16:355–363, 1997.

[29] A. Nagy. *Manipulating The Mouse Embryo: A Laboratory Manual*. Cold Spring Harbor Laboratory Pres, 2003.

[30] A. Perea-Gomez, FD. Vella, W. Shawlot, M. Oulad-Abdelghani, C. Chazaud, C. Meno, V. Pfister, L. Chen, E. Robertson, H. Hamada, RR. Behringer, and SL. Ang. Nodal antagonists in the anterior visceral endoderm prevent the formation of multiple primitive streaks. *Development Cell*, 3:745–756, 2002.

[31] D. Psychoyos and C.D. Stern. Fates and migratory routes of primitive streak cells in the chick embryo. *Development*, 122:1523–1534, 1996.

[32] M. Rhinn, A. Dierich, W. Shawlot, RR. Behringer, M. Le Meur, and Sl. Ang. Sequential roles for otx2 in visceral endoderm and neuroectoderm for forebrain and midbrain induction and specifi cation. *Development*, 125:845–856, 1998.

[33] MA. Rieger, PS. Hoppe, BM. Smejkal, AC. Eitelhuber, and T. Schroeder. Hematopoietic cytokines can instruct lineage choice. *Science*, 325:217–218, 2009.

[34] M. Schwarzfischer, C. Marr, J. Krumsiek, PS. Hoppe, T. Schroeder, and F. Theis. Effcient fuorescence image normalization for time lapse movies. 2011.

[35] B. Streppel. *Data Mining Approaches for Analyzing Single Cell Stem Cell Data*. PhD thesis, 2012.

[36] S. Tada, T. Era, C. Furusawa, H. Sakurai, S. Nishikawa, M. Kinoshita, K. Nakao, T. Chiba, and S. Nishikawa S. Characterization of mesendoderm: a diverging point of the de?nitive endoderm and mesoderm in embryonic stem cell differentiation culture. *Development*, 132:4363–4374, 2005.

[37] H . Wan, S. Dingle, Y. Xu, V. Besnard, KH. Kaestner, SL. Ang, S. Wert, MT. Stahlman, and JA. Whitsett. Compensatory roles of foxa1 and foxa2 during lung morphogenesis. *J Biol Chem*, 280:13809–13816, 2005.

[38] H. Wang and SK. Dey. Roadmap to embryo implantation: clues from mouse models. *Nat Rev Genet*, 7:185–99, 2006.

[39] Sophia Weimer. Der schmale grat der stammzellforschung. *Die Welt*, 2013.

[40] JM. Wells and DA. Melton. Early mouse endoderm is patterned by soluble factors from adjacent germ layers. *Development*, 127:1563–1572, 1999.

[41] JM. Wells and DA. Melton. Vertebrate endoderm development. *Annu Rev Cell Dev Biol*, 15:393–410, 2000.

[42] David G. Wilkinson, Sangita Bhatt, and Berhnahrd G. Herrmann. Expression pattern of the mouse t gene and its mesoderm formation. *Nature*, 15:343–657, 1990.

[43] Evan Winchester. Stem cell breakthrough: Artificial trachea implant saves toddler hannah warren's life. *Medical Daily*, 2013.

[44] KO. Yanagisawa, H. Fujimoto, and H. Urushihara. Effects of the brachyury (t) mutation on morphogenetic movement in the mouse embryo. *Development Biology*, 2:242–248, 1981.

[45] Masahiro Yasunaga, Shinsuke Tada, Satomi Torikai-Nishikawa, Yoko Nakano, Mitsuhiro Okada, Lars Martin Jakt, Satomi Nishikawa, Tsutomu Chiba, Takumi Era, and Shin-Ichi Nishikawa. Induction and monitoring of de?nitive and visceral endoderm differentiation of mouse es cells. *Nature Biotechnology*, 23:1542–1550, 2005.

[46] L. Zhang, NE. Rubins, RS. Ahima, LE. Greenbaum, and KH. Kaestner. Foxa2 integrates the transcriptional response of the hepatocyte to fasting. *Cell Metabolism*, 2:141–148, 2005.

[47] Aaron M. Zorn and James M. Wells. Vertebrate endoderm development and organ formation. *Annu Rev Cell Dev Biol*, 25:221–251, 2009.